OCEAN SWELL WITHIN THE KINETIC EQUATION FOR WATER WAVES

Sergei I. Badulin[1,2] and Vladimir E. Zakharov[1,2,3,4,5]

[1]P. P. Shirshov Institute of Oceanology of the Russian Academy of Science, Russia
[2]Novosibirsk State University, Russia
[3]University of Arizona, Tuscon, USA
[4]P.N. Lebedev Physical Institute of Russian Academy of Sciences
[5]Waves and Solitons LLC, Phoenix, Arizona, USA

Correspondence to: S. I. Badulin (badulin.si@ocean.ru)

Abstract. Results of extensive simulations of swell evolution within the duration-limited setup for the kinetic Hasselmann equation for long durations of up to $2{\cdot}10^6$ seconds are presented. Basic solutions of the theory of weak turbulence, the so-called Kolmogorov-Zakharov solutions, are shown to be relevant to the results of the simulations. Features of self-similarity of wave spectra are detailed and their impact on methods of ocean swell monitoring are discussed. Essential drop of wave energy (wave height) due to wave-wave interactions is found at initial stages of swell evolution (of order of 1000 km for typical parameters of the ocean swell). At longer times wave-wave interactions are responsible for a universal angular distribution of wave spectra in a wide range of initial conditions. Weak power-law attenuation of swell within the Hasselmann equation is not consistent with results of ocean swell tracking from satellite altimetry and SAR (Synthetic Aperture Radar) data. At the same time, the relatively fast weakening of wave-wave interactions makes the swell evolution sensitive to other effects. In particular, as shown, coupling with locally generated wind waves can force the swell to grow at relatively light winds.

1 Physical models of ocean swell

Ocean swell is an important constituent of the field of surface gravity waves in the sea and, more generally, of the sea environment as a whole. Swell is usually defined as a fraction of wave field that does not depend (or depends slightly) on local wind. Being generated in confined stormy areas these waves can propagate long distances of many thousand miles, thus, influencing vast ocean stretches. For example, swell from Roaring Forties in the Southern Ocean can traverse the Pacifica and reach distant shores of California and Kamchatka. Predicting of swell as a part of sea wave forecast remains a burning problem for maritime safety and marine engineering.

Pioneering works by Barber and Ursell (1948); Munk et al. (1963); Snodgrass et al. (1966) discovered a rich physics of the phenomenon and gave first examples of accurate measurements of magnitudes, periods and directional spreading of swell. All the articles contain thorough discussions of physical background of swell generation, attenuation and interaction with other types of ocean motions. Nonlinear wave-wave interactions have been sketched by Snodgrass et al. (1966) as a novelty introduced by the milestone papers by Phillips (1960) and Hasselmann (1962). A possible important role of these interactions

at high swells for relatively short time of evolution has been outlined and evaluated. The first estimates of the observed rates of swell attenuation have been carried out by Snodgrass et al. (1966) based on observation at near-shore stations. Their e-folding scale about 4000 km (distance in which an exponentially decaying wave height decreases by a factor of e) is consistent with some of today's results of the satellite tracking of swell (Ardhuin et al., 2009, 2010; Jiang et al., 2016) and with treatment of these results within the model of swell attenuation due to coupling with turbulent atmospheric layer (e.g. Kantha, 2006). Alternative semi-empirical model of Babanin (2006) predicts quite different algebraic law and stronger swell attenuation at shorter distances from the swell source (Young et al., 2013). Note that the effect of the decay of a monochromatic wave due to turbulent wave flow is found to be quadratic in wave amplitude, i.e. to be of lower-order nonlinearity than in the non-dissipative theory of weakly nonlinear water waves (cubic nonlinearity). It makes questionable an incorporating of the model into the today statistical (and even dynamical) theories of sea waves that account for the effect of intrinsic wave nonlinearity.

It should be stressed that all the mentioned models treat swell as a quasi-monochromatic wave and, thus, ignore nonlinear interactions of the swell harmonics themselves and the swell coupling with locally generated wind waves. The latter effect can be essential as observations and simulations clearly show (e.g. Kahma and Pettersson, 1994; Pettersson, 2004; Young, 2006; Badulin et al., 2008b, and refs. therein). At most the swell is continuing to be considered as a superposition of harmonics that do not interact with each other and, thus, can be described by the well-known methods of the linear theory of waves (e.g. Ewans, 1998; Ewans et al., 2004). Many features of the observed swell can be related to such models. For example, the observed effect of linear growth of the swell frequency in a site can be explained as an effect of dispersion of a linear wave packet over long time and successfully used for relating these observations with stormy areas that generate the swell (e.g. Barber and Ursell, 1948; Ewans et al., 2004).

Synthetic aperture radars (SAR) allow for spatial resolution up to tens of meters (e.g. Ardhuin et al., 2010; Young et al., 2013). Satellite altimeters measure wave height averaged over a snapshot of a few square kilometers. These snapshots are adequate for currently known methods of statistical description of waves in research and application models. These can be used for swell tracking in combination with other tools (e.g. wave models as in Jiang et al., 2016). Re-tracking of swells allows, first, for relating the swell events with their probable sources – stormy areas and, secondly, the swell transformation gives a clue to estimating effects of other motions of the atmosphere and ocean – seasonal wind activity (e.g. Chen et al., 2002), wave-current interaction (e.g. Beal et al., 1997) and bathimetry effects (Young et al., 2013) etc. Such work requires adequate physical models of swell propagation and transformation as far as the number of parameters of sea environment remains beyond our control.

Meanwhile, the linear treatment remains quite restrictive and cannot explain important features of swell. The observed swell spectra exhibit frequency downshift which is not predicted by deterministic linear or weakly nonlinear models of narrow-banded wave guide evolution (e.g. data of Snodgrass et al., 1966, and comments on these data by Henderson and Segur (2013)). Moreover, these spectra show invariance of their shapes that is unlikely to appear in linear dispersive wave system. These noted features are common for wave spectra described by the kinetic equation for water waves, the so-called Hasselmann (1962) equation.

In this paper we present results of extensive simulations of ocean swell within the Hasselmann equation for deep water waves. The simplest duration-limited setup has been chosen to obtain numerical solutions for the duration up to $2 \cdot 10^6$ seconds (about 23 days) for typical parameters of ocean swell (wavelengths $150 - 400$ meters, wave periods $10 - 16$ s, initial significant heights $3 - 15$ meters).

We analyze the simulation results from the viewpoint of the theory of weak turbulence (Zakharov et al., 1992). The slowly evolving swell solutions appear to be quite close to the stationary milestone Kolmogorov-Zakharov solutions for water waves in a frequency range (Zakharov and Filonenko, 1966; Zakharov and Zaslavsky, 1982). We give a short theoretical introduction and present estimates of the basic constants of the theory in the next section. In sect.3 we relate results of simulations with properties of the self-similar solutions of the kinetic equation. Zaslavskii (2000) was the first to present the self-similar solutions for swell assuming the angular narrowness of the swell spectra and stated explicit analytical results. In fact, more general consideration, in the spirit of Badulin et al. (2002, 2005a), leads to important findings and raises questions independent of the assumption of angular narrowness.

We demonstrate the well-known fact that is usually ignored: the power-law swell attenuation within the conservative kinetic equation. We show that it does not contradict results of observations mentioned above. We also reveal a remarkable feature of collapsing the swell spectra onto an angular distribution that depends weakly on initial angular spreading. Such universality can be of great value for modelling swell and developing methods for its monitoring (Delpey et al., 2010).

We conclude this paper with a discussion of how to apply this model. Evidently, the setup of duration-limited evolution is quite restrictive and does not reflect essential features of ocean swell when wave dispersion and spatial divergence play a key role. At the same time, wave-wave interactions remain of importance independently of the setup. The weakening of swell evolution is not directly related to abatement of wave-wave interactions which are able to effectively restore perturbations of these quasi-stationary states (Zakharov and Badulin, 2011). On the contrary, this favors coupling of the quasi-stationary swell with ocean environment. In particular, the locally generated wind-driven waves can switch the swell attenuation to swell amplification. This effect can be considered for interpretation of recent observations of swell from space ('negative' dissipation in words of Jiang et al., 2016). Many problems of adequate physical description of swell in the ocean are still open. This paper is an attempt to reveal essential features of swell evolution within the simplest model of the kinetic Hasselmann equation.

2 Solutions for ocean swell

2.1 The Kolmogorov-Zakharov solutions

In this section we reproduce previously reported theoretical results on evolution of swell as a random field of weakly interacting wave harmonics. We apply the statistical theory of wind-driven seas (Zakharov, 1999) to the sea swell, whose description with this approach, is usually considered questionable. A random wave field is described by the kinetic equation derived by Klauss Hasselmann (1962) for weakly nonlinear deep water waves in the absence of dissipation and external forcing

$$\frac{\partial N_{\mathbf{k}}}{\partial t} + \nabla_{\mathbf{k}} \omega_{\mathbf{k}} \nabla_{\mathbf{r}} N_{\mathbf{k}} = S_{nl}. \tag{1}$$

Equation (1) is written for the spectral density of wave action $N(\mathbf{k},\mathbf{x},t) = E(\mathbf{k},\mathbf{x},t)/\omega(\mathbf{k})$ ($E(\mathbf{k},\mathbf{x},t)$ is the wave energy spectrum and the wave frequency obeys linear dispersion relation $\omega = \sqrt{g|\mathbf{k}|}$). Subscripts for ∇ corresponds to the two-dimensional gradient operator in the corresponding space of coordinates $\mathbf{x}$ and wavevectors $\mathbf{k}$ (i.e. $\nabla_{\mathbf{r}} = (\partial/\partial x, \partial/\partial y)$).

The right-hand term S_{nl} describes the effect of wave-wave resonant interactions and can be written in explicit form (see Appendices in Badulin et al., 2005a, for collection of formulas). The cumbersome term S_{nl} causes many problems for wave modelling whenever (1) is extensively used. Nevertheless, for the deep water case, one has a key property of homogeneity

$$S_{nl}[\kappa\mathbf{k}, \upsilon N_{\mathbf{k}}] = \kappa^{19/2}\upsilon^3 S_{nl}[\mathbf{k}, N_{\mathbf{k}}]. \tag{2}$$

that helps in acquiring important analytical results. Stretching in κ times in wave scale or in υ times in wave action, where κ, υ are positive leads to simple re-scaling of the collision term, S_{nl}. This important property gives a clue for constructing power-law stationary solutions of the kinetic equation, i.e. solutions for the equation

$$S_{nl} = 0. \tag{3}$$

Two isotropic stationary solutions of (3) correspond to constant fluxes of wave energy and action in wave scales. The direct cascade solution (Zakharov and Filonenko, 1966) in terms of frequency spectrum of energy

$$E^{(1)}(\omega,\theta) = 2C_p \frac{P^{1/3} g^{4/3}}{\omega^4} \tag{4}$$

introduces the basic Kolmogorov constant C_p and describes the energy transfer to infinitely short waves with constant flux P. The wave action transfer in the opposite direction of long waves is described by the inverse cascade solution (Zakharov and Zaslavsky, 1982) with wave action flux Q and another Kolmogorov's constant C_q:

$$E^{(2)}(\omega,\theta) = 2C_q \frac{Q^{1/3} g^{4/3}}{\omega^{11/3}}. \tag{5}$$

An approximate weakly anisotropic Kolmogorov-Zakharov solution has been obtained by Katz and Kontorovich (1974) as an extension of (4)

$$E^{(3)}(\omega,\theta) = 2\frac{P^{1/3} g^{4/3}}{\omega^4}\left(C_p + C_m \frac{gM}{\omega P}\cos\theta + \dots\right). \tag{6}$$

It associates the wave spectrum anisotropy with the constant spectral flux of wave momentum M and the so-called second Kolmogorov constant C_m. As it is seen from (6) the solution anisotropy vanishes as $\omega \to \infty$: wave spectra become isotropic for short waves. The whole set of the KZ solutions (4–6) can be treated naturally within the dimensional approach: these are just particular cases of solutions of the form

$$E^{(KZ)}(\omega) = \frac{P^{1/3} g^{4/3}}{\omega^4} G(\omega Q/P, gM/(\omega P), \theta) \tag{7}$$

where G is a function of dimensionless arguments scaled by spectral fluxes of wave energy P, action Q and momentum M.

Originally, solutions (4–6) were derived in particularly sophisticated and cumbersome ways. Later on, simpler and more physically transparent approaches have been presented (Zakharov and Pushkarev, 1999; Balk, 2000; Pushkarev et al., 2003,

2004; Badulin et al., 2005a; Zakharov, 2010). These more general approaches allow for looking at higher-order terms of the anisotropic Kolmogorov-Zakharov solutions (6). In particular, they predict the next term proportional to $\cos 2\theta/\omega^2$ which is the second angular harmonics of the stationary solution (6).

Swell solutions evolve slowly with time and, thus, give a good opportunity for discussing features of the KZ solutions (or, alternatively, the KZ solutions can be used as a reference case for the swell studies). One of the key points of this discussion is the question of uniqueness, universality of the swell solutions that can be treated in the context of general KZ solutions (7). The principal terms of the general Kolomogorov-Zakharov solutions (4–6) have clear physical meaning of total fluxes of wave action (5), energy (4) and momentum (6) and do not refer to specific initial conditions. This is not the case for the higher-order terms. The link between these additional terms with inherent properties of the collision integral S_{nl} and/or with specific initial conditions is a subject of special study.

2.2 Self-similar solutions of the kinetic equation

The homogeneity property (2) is extremely useful for studies of non-stationary (inhomogeneous) solutions of the kinetic equation. Approximate self-similar solutions for reference cases of duration- and fetch-limited development of wave field can be obtained under the assumption of dominance of the wave-wave interaction term S_{nl} (Pushkarev et al., 2003; Zakharov, 2005; Badulin et al., 2005a; Zakharov and Badulin, 2011). These solutions have forms of the so-called incomplete or the second type self-similarity (e.g. Barrenblatt, 1979). In terms of frequency-angle dependencies of wave action spectra one has for the duration- and fetch-limited cases correspondingly (Badulin et al., 2005a, 2007; Zakharov et al., 2015)

$$N(\omega,\theta,\tau) = a_\tau \tau^{p_\tau} \Phi_{p_\tau}(\xi,\theta) \tag{8}$$

$$N(\omega,\theta,\chi) = a_\chi \chi^{p_\chi} \Phi_{p_\chi}(\zeta,\theta) \tag{9}$$

with dimensionless time τ and fetch χ

$$\tau = t/t_0; \qquad \chi = x/x_0. \tag{10}$$

Dimensionless arguments of shape functions $\Phi_{p_\tau}(\xi)$, $\Phi_{p_\chi}(\zeta)$ in (8,9) contain free scaling parameters b_τ, b_χ and exponents of frequency downshifting q_τ, q_χ

$$\xi = b_\tau \omega^2 \tau^{-2q_\tau}; \qquad \zeta = b_\chi \omega^2 \chi^{-2q_\chi}. \tag{11}$$

Homogeneity properties (2) dictates 'magic relations' (in the words of Pushkarev and Zakharov, 2015, 2016) between exponents p_τ, q_τ and p_χ, q_χ

$$p_\tau = \frac{9q_\tau - 1}{2}; \qquad p_\chi = \frac{10q_\chi - 1}{2}. \tag{12}$$

Additional 'magic relations' coming from homogeneity property (2) fix a link between the amplitude scales a_τ, a_χ and the bandwidth scales b_τ, b_χ of the self-similar solutions (8–11)

$$a_\tau = b_\tau^{19/4}; \qquad a_\chi = b_\chi^{5/2}. \tag{13}$$

Thus, 'magic relations' (12,13) reduce number of free parameters of the self-similar solutions (8,9) from four (two exponents and two coefficients) to two only: a dimensionless exponent $p_\tau\,(p_\chi)$ and an amplitude of the solution $a_\tau\,(a_\chi)$.

The shape functions $\Phi_\tau(\xi), \Phi_\chi(\zeta)$ in (8,9) are specified by solutions of a boundary problem for an integro-differential equation in self-similar variable ξ (or ζ for fetch-limited case) and angle θ (see sect. 5.2 Badulin et al., 2005a, for details). Simulations (e.g. Badulin et al., 2008a) reveal remarkable features of the shape functions $\Phi_\tau(\xi), \Phi_\chi(\zeta)$. Numerical solutions generally show relatively narrow angular distributions for $\Phi_{p_\tau}(\xi), \Phi_{p_\chi}(\zeta)$ with a single pronounced maximum at a spectral peak frequency ω_p. This implies that the only one (or very few) of an infinite series of eigenfunctions of the boundary problem for the shape functions $\Phi_{p_\tau}(\xi), \Phi_{p_\chi}(\zeta)$ contributes to wave spectra evolution in a wide range of initial and external forcing conditions. This treatment of the heavily nonlinear boundary problem in terms of a composition of eigenfunctions is possible in this case as demonstrated by Zakharov and Pushkarev (1999). Two-lobe patterns can be observed beyond the spectral peak as local maxima at oblique directions or as a 'shoulder' in wave frequency spectra. Their appearance within the kinetic equation approach is generally associated with wind generation (e.g. Bottema and van Vledder, 2008, 2009) and/or effect of wave-wave interactions (Pushkarev et al., 2003). Numerical simulations within the potential Euler equations also show formation of the two-lobe patterns for rather short times (very few hundreds of spectral peak periods) of evolution of initially unimodal spectral distribution (Toffoli et al., 2010).

An important property of *spectral shape invariance* (terminology of Hasselmann et al., 1976) or *the spectra quasi-universality* (in the words of Badulin et al., 2005a) is widely discussed both for experimentally observed and simulated wave spectra. This invariance does not suppose a point-by-point coincidence of properly normalized spectral shapes. Proximity of integrals of the shape functions $\Phi_{p_\tau}, \Phi_{p_\chi}$ in a range of wave growth rates p_τ, p_χ appears to be sufficient for formulating a remarkable universal relationship for parameters of self-similar solutions (8,9)

$$\mu^4\nu = \alpha_0^3. \tag{14}$$

Here wave steepness μ is estimated from total wave energy E and spectral peak frequency ω_p

$$\mu = \frac{E^{1/2}\omega_p^2}{g}. \tag{15}$$

The 'number of waves' ν in a spatially homogeneous wind sea (i.e. for duration-limited case) is defined as follows:

$$\nu = \omega_p t. \tag{16}$$

For spatial (fetch-limited) wave growth, the coefficient of proportionality C_f in the equivalent expression $\nu = C_f|\mathbf{k}_p|x$ ($\mathbf{k}_p$ being the wavevector of the spectral peak) is close to the ratio between the phase and group velocities $C_{ph}/C_g = 2$. A universal constant $\alpha_0 \approx 0.7$ is a counterpart of the constants C_p, C_q of the stationary Kolmogorov-Zakharov solutions (4,5) and has a similar physical meaning of a ratio between wave energy and the energy spectral flux (in power $1/3$). A remarkable feature of the universal wave growth law (14) is its independence of wind speed. This wind-free paradigm based on intrinsic scaling of wave development is shown to be a useful tool of analysis of wind-wave growth (Zakharov et al., 2015). Below we demonstrate its effectiveness for results of swell simulations.

2.3 Self-similarity of swell solutions

The self-similar solution for swell is just a member of a family of solutions (8,9) with special values of temporal or spatial rates

$$p_\tau = 1/11; \qquad q_\tau = 1/11 \tag{17}$$

$$p_\chi = 1/12; \qquad q_\chi = 1/12 \tag{18}$$

Exponents (17,18) provide conservation of the total wave action for its evolution in time (duration-limited setup) or in space (fetch-limited)

$$N = \int_0^\infty N(\omega,\theta)d\omega d\theta = \text{const} \tag{19}$$

On the contrary, total energy

$$E = \int \omega N(\mathbf{k})d\mathbf{k} \tag{20}$$

and wave momentum

$$\mathbf{K} = \int \mathbf{k} N(\mathbf{k})d\mathbf{k} \tag{21}$$

are only formal constants of motion of the Hasselmann equation and decay with time t or fetch x

$$E \sim t^{-1/11}; \qquad K_x \sim t^{-2/11} \tag{22}$$

$$E \sim x^{-1/12}; \qquad K_x \sim x^{-2/12}. \tag{23}$$

The swell decay (22,23) reflects a basic feature of the kinetic equation for water waves: energy (20) and momentum (21) are not conserved (see Zakharov et al., 1992; Pushkarev et al., 2003, and refs. herein). The wave action is the only true integral of the kinetic equation (1).

The swell solution manifests another general feature of evolving spectra: the downshifting of the spectral peak frequency (or other characteristic frequency), i.e.

$$\omega_p \sim t^{-1/11}; \qquad \omega_p \sim x^{-1/12}. \tag{24}$$

The universal law of wave evolution (14) is, evidently, valid for the self-similar swell solution as well with a minor difference in the value of the constant α_0. As soon as this constant is expressed in terms of the integrals of the shape functions Φ_τ, Φ_χ and the swell spectrum shape differs essentially from ones of the growing wind seas, this constant appears to be less than α_0 of the growing wind seas.

The theoretical background presented above is used below for analysis of results of simulations.

3 Swell simulations

3.1 Simulation setup

Simulations of ocean swell require special care. First of all, calculations for quite long periods of time (up to $2 \cdot 10^6$ seconds in our case) should be accurate enough in order to capture relatively slow evolution of solutions and, thus, be able to relate results with the theoretical background presented above. Duration-limited evolution of the swell has been simulated with the Pushkarev et al. (2003) version of the code based on the WRT algorithm (Webb, 1978; Tracy and Resio, 1982). Features of the code and numerical setups have been described in previous papers (Badulin et al., 2002; Badulin and A. N. Pushkarev, 2004; Badulin et al., 2005a, b, 2007; Zakharov et al., 2007; Badulin et al., 2008a, 2013; Pushkarev and Zakharov, 2015, 2016). Frequency resolution for log-spaced grid has been set to $(\omega_{n+1} - \omega_n)/\omega_n = 1.03128266$. It corresponds to 128 grid point in frequency range $0.02 - 1$ Hz (approximately 1.5 to 3850 meters wave length).

Standard angular resolution $\Delta\theta = 10^\circ$ has been taken as adequate for the goals of our study. A control series of runs with angular resolution $\Delta\theta = 5^\circ$ showed very close but still quantitatively different shaping of wave spectra (see discussion below) while differences of integral parameters (wave height, period, total momentum) did not exceed 1% after 10^6s of evolution.

Initial conditions were similar in all series of simulations: spectral density of action in wavenumber space was almost constant in a box of the wavenumber modulo and angles. Slight modulation (5% of the box height) and low pedestal outside the box (six orders less than the maximal value) have been set in order to stimulate wave-wave interactions since the collision integral S_{nl} vanishes for $N(\mathbf{k}) = \mathrm{const}$:

$$N(\mathbf{k}) = \begin{cases} N_0(1 + 0.05\cos^2(\theta/2)), |\theta| < \Theta/2, \omega_l < \omega < \omega_h \\ 10^{-6} N_0, \qquad \text{otherwise} \end{cases} \tag{25}$$

In (25) the references to angle θ ($\cos\theta = k_x/|\mathbf{k}|$) and wave frequency ω are used for conciseness of the expression for spatial wave action spectrum $N(\mathbf{k})$. The default values ω_l and ω_h corresponding to wave periods 10 and 2.5s have been used for the most cases providing sufficient space for spectral evolution to low frequencies (spectra downshifting) and for stability of calculations at high frequencies for the default cutoff frequency $f_c = 1$Hz.

Dissipation was absent in the runs. Free boundary conditions were applied at the high-frequency end of the domain of calculations: generally, short-term oscillations of the spectrum tail do not lead to instability, i.e. the resulting solutions can be regarded as ones corresponding to conditions of decay at infinitely small scales ($N(\mathbf{k}) \to 0$ when $|\mathbf{k}| \to \infty$).

Calculations with a hyper-dissipation (e.g. Pushkarev et al., 2003) or a diagnostic tail at the high-frequency range of the spectrum (Gagnaire-Renou et al., 2010) do not affect results quantitatively compared to our other simulations. Very strong dissipation at less than 10 grid points at the very end of frequency domain suppresses spectral level and, simultaneously, reduces the overall energy dissipation at these points. Thus, the effect on the evolution of the energy-containing part of the solution appears to be quite weak and depends slightly on particular form and magnitude of the hyper-dissipation. In some cases, the hyper-dissipation option that suppresses high-frequency noise can accelerate calculations. In a sense, it is equivalent

to reducing an effective number of grid points. Test runs with the reduced frequency domain (cutoff up to $f_c = 0.6$Hz, 112 grid points) did not show essential quantitative difference with the default option ($f_c = 1$Hz, 128 grid points).

In contrast to wind-driven waves where wind speed is an essential physical parameter that gives a useful physical scale, the swell evolution is determined by initial conditions only, i.e. by N_0 (dimension of wave action spectral density $[N(\mathbf{k})] = [\text{Length}^4 \cdot \text{Time}]$), a characteristic frequency (sideband $[\omega_l, \omega_h]$) and angular spreading Θ within the setup (25). We tried different combinations of these parameters. Three frequency bands $[0.026 - 0.09]$, $[0.058 - 0.25]$, $[0.1 - 0.4]$ Hz have been chosen to generate swell with wavelengths approximately $200, 300, 400$ meters at final stages of evolution. The angular spreading Θ was set at $30°$, $50°$, $170°$, $230°$ and $330°$. Initial significant wave heights H_s were taken as approximately $4.8, 8, 10, 12, 18$ meters. As it will be detailed below an abrupt fall of wave energy occurred at the very first hours of evolution (up to 50% for the first 1 hour). Thus, the above high values of H_s can be accepted as realistic values for sea swell. Totally, more than 30 combinations of wave height, frequency range and angular spreading have been simulated successfully for the duration at least 10^6 s. In some cases, for high amplitudes and narrow angular spreadings, simulations have failed because of strong numerical instability.

Below we focus ourselves on the series of Table 1 where initial wave heights were fixed (within 2%) at approximately 4.8 meters and angular spreading varied from very narrow $\Theta = 30°$ to almost isotropic $\Theta = 330°$ (25). The frequency range of the initial perturbations was $0.1 - 0.4$Hz. The simulations has been carried out for duration $2 \cdot 10^6$ seconds with angular resolution $\Delta\theta = 10°$ and checked for series `sw030` and `sw330` with $\Delta\theta = 5°$.

3.2 Self-similarity features of swell

Evolution of swell spectra with time is shown in fig.1 for the case `sw330` of Table 1. The example shows a strong tendency to self-similar shaping of wave spectra. This remarkable feature has been demonstrated and discussed for swell in previous works (Badulin et al., 2005a; Benoit and Gagnaire-Renou, 2007; Gagnaire-Renou et al., 2010) for special parameters that provided relatively fast evolution of rather short and unrealistically high waves. In our simulations, we start with the mean wave period of about 3 seconds that corresponds to the end of calculations of Badulin et al. (2005a, see fig. 8 therein) and moderately high steepness $\mu \approx 0.15$ as defined by (15). The initial step-like spectrum evolves very quickly and keeps a characteristic shape for less than 1 hour. For 555 hours the spectral peak period reaches 11.4 seconds (the corresponding wavelength $\lambda \approx 200$ meters) and wave steepness becomes $\mu = 0.022$. The final significant wave height $H_s \approx 2.8$ meters is essentially less than its initial value 4.8 meters. All these values can be considered as typical ones for ocean swell.

Dependence of key wave parameters on time is shown in fig. 2 for different runs of Table 1. Power-law dependencies of self-similar solutions (17,18,22-24) are shown by dashed lines. In fig. 2*a,b* total wave energy E and the spectral peak frequency ω_p show good correspondence to power laws of the self-similar solutions (8). By contrast, power-law decay of $x-$component of wave momentum K_x depends essentially on angular spreading of initial wave spectra. While for narrow spreading (runs `sw030` and `sw050`) there is no visible deviation from the $K_x \sim t^{-2/11}$ law, wide-angle cases clearly show these deviations. The 'almost isotropic' solution for `sw330` is tending quite slowly to the theoretical dependency of wave momentum K_x (23). The duration more than 3 weeks appears 'too short': one can see a transitional behavior when wave spectra evolve from the 'almost isotropic' state to an inherent distribution with a pronounced anisotropy.

A simple quantitative estimate of the 'degree of anisotropy' is given in fig.2*d*. Evolution of dimensionless parameter of anisotropy in terms of the approximate Kolmogorov-Zakharov solution (6) by Katz and Kontorovich (1974) is shown for all the cases of Table 1. We introduce parameter of anisotropy A as follows

$$A = \frac{gM}{\omega_p P}. \tag{26}$$

where total energy flux P (energy flux at $\omega \to \infty$) is estimated from evolution of total energy

$$P = -\frac{dE}{dt}. \tag{27}$$

Similarly, total wave momentum (21) provides an estimate of its flux as follows

$$M = -\frac{dK_x}{dt}. \tag{28}$$

Spectral peak frequency ω_p has been used for the definition of 'degree of anisotropy', A (26). Different scenarios are seen in fig. 2*d* depending on angular spreading of wave spectra. Nevertheless, a general tendency to a universal behavior at very large times (more than $2 \cdot 10^6$ seconds) looks quite plausible.

Similar dispersion of runs depending on anisotropy of initial distributions is seen in fig. 3 when tracing the invariant of the self-similar solutions (14). Again, like in fig.2b, $2 \cdot 10^6$ seconds are not sufficient to demonstrate validity of relationship (14) in its full. A limit α_0 (14) is very likely reached at larger times. This limit is a bit less (by approximately 15%) than one for growing wind seas $\alpha_0 \approx 0.7$. Again, the 'almost isotropic' solution shows its stronger departure from the rest of the series. The differences are better seen in angular distributions rather than in normalized spectral shapes (fig. 4) when we are trying to check self-similarity features of the solutions in the spirit of Badulin et al. (2005a); Benoit and Gagnaire-Renou (2007).

3.3 Directional spreading of swell spectra

Despite significant difference of the runs in integral characteristics of the swell anisotropy (e.g. figs. 2*b,d*), the resulting spectral distributions still show pronounced features of universality as it is seen in frequency spectra (fig.4). As it will be shown below this universality of swell spectra is seen in angular distributions as well. This is of importance in the context of remarks of sect.2.2: while the shape functions Φ_{p_τ}, Φ_{p_χ} of self-similar solutions (8,9) are not unique there is likely a mechanism of their selection that supports the universality of the swell spectral distributions. Within a linear theory, it could be treated as survival of the only eigenfunction or, more prudently, of very few eigenmodes of the problem. As mentioned in sect.2.2. this 'linear' treatment can be used with some reservations for our problem which is heavily nonlinear in terms of wave spectra but allows for a quasi-linear analysis in terms of spectral fluxes (see Zakharov and Pushkarev, 1999; Pushkarev et al., 2003).

The only physical mechanism of the mode selection in the swell problem is nonlinear relaxation to an inherent state due to four-wave resonant interactions. This relaxation generally occurs at essentially shorter scales than ones of wind pumping and wave dissipation (Zakharov and Badulin, 2011). There is no contradiction with the today vision of the sea wave balance in the above statement. The effect of nonlinear interactions on wave spectra is two-fold: firstly, it supports an inherent shaping of the

spectra by very fast feedback to its perturbation and, secondly, it is responsible for relatively slow nonlinear cascading within this inherent shaping.

Normalized sections of spectra at the peak frequency ω_p are shown in fig.5 for runs of Table 1 at $t = 10^6$ seconds (approx. 11.5 days). 'The almost isotropic' run `sw330` shows relatively high pedestal of about 2% of maximal value while other series have a background one more order less. At the same time, the core of all distributions is quite close to a gaussian shape

$$y_{gauss} = \exp\left(-\frac{\theta^2}{2\sigma^2}\right) \tag{29}$$

with half-width $\sigma = 35^\circ$ (dashed curve in fig.5). Experimentally based spreading functions are represented in fig.5 by two reference curves. For growing wind seas the dependence by Donelan et al. (1985, eq.9.2)

$$y_{1985} = \mathrm{sech}^2(\beta\theta); \quad \beta = 2.28 \tag{30}$$

gives almost twice narrower distribution (dot line in fig.5).The wrapped-normal fit of angular distribution for one of the case of the West Africa Swell Project (see Table 11.2 and fig.11.8 in Ewans et al., 2004) with standard deviation $\sigma \approx 14.3^\circ$ gives a sharper distribution shown by a dashed curve.

Evolution of directional spreading in time is shown in absolute values in fig. 6 for three runs: the most anisotropic case `sw030` (fig. 6*a,b*), weakly anisotropic initial state `sw230` (fig. 6*c,d*) and 'the almost isotropic' run `sw330` (fig. 6*e,f*). In the left column the angular spreading at peak frequency shows remarkably close patterns for the first two cases: peak values at large times differ by few percents only. The weakly anisotropic case `sw230` (initial angular spreading 230° with essential counter-propagating fraction) reaches its almost saturated state for a couple of days only (cf. curves at $t = 17$ and $t = 35$ hours). Similar proximity of these two cases can be observed for integrals of spectra in frequency as shown in the right column of fig.6, i.e. for values

$$\mathcal{E}(\theta) = \int_0^{\omega_c} E(\omega,\theta)d\omega. \tag{31}$$

Self-similar solutions (8) predict a power-law decay of magnitude of $\mathcal{E}$ with time which is what we see in fig.6*b,d* for the first two cases. Behavior of 'the almost isotropic' case `sw330` is qualitatively different. The relatively strong adjustment to a narrow directional spreading occurs in course of all the duration $2 \cdot 10^6$ s. The duration appears to be too short to reach a self-similar regime resembling cases `sw030`, `sw230`.

The effect of sharpening of angular distributions of the run `sw330` in fig.6*e,f* requires additional comments. First, it manifests a transitional nature of the case `sw330` when a solution is rather far from its self-similar asymptotics. Secondly, this case illustrates the above statement of the paragraph on two scales of wave spectra evolution. The angular adjustment occurs at relatively short temporal scales as compared with slow evolution of integral parameters (cf. fig.2). This adjustment is provoked by excursion of initially 'almost isotropic' distribution from an anticipated 'inherent state' that, thus, stimulates wave-wave interactions as a mechanism of relaxation. The example demonstrates ability of wave-wave interactions to effectively rebuild directional distributions. Note, that in some cases, say, in the problem of relaxation of wave field to sudden changes of wind

direction the wave-wave interactions are considered as ineffective as compared to relaxation 'due mainly to imbalance $S_{in} < S_{diss}$' (e.g. Young et al., 1987, S_{in} – wind input, S_{diss} – wave dissipation).

3.4 Bi-modality of swell spectra

Bi-modality of directional spreading of ocean swell is widely discussed for experimental data as a possible result of swell evolution (e.g. Ewans, 1998, 2001; Ewans et al., 2004). Our simulations encounter this effect as a persistent feature of swell spectra. Fig.7 represents directional spreading of swell spectra in two ways. The left column shows directional distribution function $H(\omega,\theta)$ in the spirit of widely used definition (e.g. Ewans, 1998)

$$E(\omega,\theta) = \bar{E}(\omega)H(\omega,\theta), \quad H(\omega,\theta) \geq 0, \quad \int_{-\pi}^{\pi} H(\omega,\theta)d\omega = 1. \tag{32}$$

An alternative representation in the right column of fig.7 uses spectral densities normalized by their maxima at fixed frequency to trace 'ridges' of surface $\tilde{E}(\omega,\theta)$ defined as follows (cf. eq.1 in Young et al., 1995)

$$\tilde{E}(\omega,\theta) = E(\omega,\theta)/\max_{-\pi<\theta\leq\pi}(E(\omega,\theta)). \tag{33}$$

Both representations reveal bi-modality of swell spectra fairly well for all cases of Table 1. 'Narrow' initial spectrum `sw030` and 'wide' one `sw170` evolves to very close X-shaped side-lobe patterns (fig.7*a,c*). Pronounced side-lobes are seen both above and below the spectral peak frequency. Directional distribution function $H(\omega,\theta)$ (32) does not show similar pattern for 'the almost isotropic' case `sw330` (fig.7*e,g*) but the X-shapes are seen fairly well in the 'ridge' representation (33) for all the cases. Directional spreading for the run `sw330` is shown for simulations with standard angular resolution $\Delta\theta = 10^\circ$ (fig.7*e,f*) and with fine one $\Delta\theta = 5^\circ$ (fig.7*g,h*). Higher resolution makes 'ridges' sharper and allows for resolving more details of the directional distribution. In particular, side-lobes appear for counter-propagating waves at $\theta \approx \pm 3\pi/4$ and $\omega/\omega_p \approx 5/4$. At the same time, the standard angular resolution in our simulations $\Delta\theta = 10^\circ$ seems to be adequate for the bi-modality phenomenon.

The patterns similar to ones of fig.7 have been obtained in simulations of the Hasselmann equation for wind-driven waves with the exact term of nonlinear transfer S_{nl} by Banner and Young (1994b); Young et al. (1995) at formally finer resolution $\Delta\theta = 6.67^\circ$. It should be noted that directions beyond the cone $\theta = \pm 120^\circ$ have not been taken into account to speed up calculations in the cited papers. It can explain discrepancy with our results at the high frequency end of fig.7*f,h* (cf. Plate 1 in Young et al., 1995). This point can be clarified in further studies.

An important issue of agreement of our results and findings of Banner and Young (1994b); Young et al. (1995) is presence of low-frequency (below the spectral peak) side-lobes. Experimental results by Ewans (cf. figs.8,16 1998) show good correspondence of the directional spreading functions with numerical results at high frequencies but do not fix any side-lobes below the spectral peak.

Generally, the phenomenon of side-lobe occurrence is associated with a joint effect of wave-wave interactions and wind generation (e.g. Banner and Young, 1994b; Pushkarev et al., 2003; Bottema and van Vledder, 2008). The theoretical background of sect. 2.1 and our simulations of swell can propose an interpretation and alternative ways of advanced analysis of the effect in

terms of stationary solutions of Kolmogorov-Zakharov (7). These solutions being presented as power series of dimensionless ratios of spectral fluxes and as an extension of the approximate solution (6) by Katz and Kontorovich (1974) predict higher-order angular harmonics and can be found within the formal procedure of Pushkarev et al. (2003, 2004). This approach is not fully correct in the vicinity of the spectral peak but still looks plausible and useful for interpretation of the effect of wave-wave interactions. Analysis of the next paragraph shows perspectives of the KZ solution paradigm.

3.5 Swell spectra vs KZ solutions

Very slow evolution of swell in our simulations provides a chance to check relevance of the classic Kolmogorov-Zakharov solutions (4-7) to the problem under study. The key feature of the swell solution from the theoretical viewpoint is its 'hybrid' (in the words of Badulin et al., 2005a) nature: inverse cascade (negative fluxes) determines evolution of spectral peak and its downshifting while the direct cascade (positive fluxes) occurs at frequencies slightly (approximately 20%) above the peak. This hybrid nature is illustrated by fig. 8 for energy and wave momentum fluxes. In order to avoid ambiguity in treatment of the simulation results within the weak turbulence theory we will not discuss this hybrid nature of swell solutions and focus on the direct cascade regime. Thus, general solution (7) in the form

$$E(\omega,\theta) == \frac{P^{1/3}g^{4/3}}{\omega^4}G(0,gM/(\omega P),\theta)$$

and its approximate explicit version (6) by Katz and Kontorovich (1971, 1974) will be used below for describing the direct cascading of energy and momentum at high frequency (as compared to ω_p) .

Two runs of Table 1, `sw030` and 'almost isotropic' `sw330`, are presented in fig.8 in order to show qualitative similarity of extreme cases of initial directional spreading. Positive fluxes P and M decays with time in good agreement with power-law dependencies (22) and have rather low variations in relatively wide frequency range $3\omega_p < \omega < 6\omega_p$ in fig. 8. For energy fluxes P (figs.8*a,b*) one can see good quantitative correspondence (note, that times for some curves are slightly different). Absolute values of momentum flux M as well as magnitudes of wave momentum itself (see fig.2) differ by more than one order.

The domain of quasi-constant fluxes $\omega > 3\omega_p$ can be used for verification of relevance of the stationary KZ solutions (4–6) to the quasi-stationary swell solutions. All the cases of Table 1 show very close patterns of spectral fluxes (e.g. fig.8) and, what is more important, very close estimates of Kolmogorov's constants.

The first and the second Kolmogorov's constants can be easily estimated for the approximate solution (6) from combinations of along- and counter-propagating spectral densities as follows

$$C_p = \frac{\omega^4\left(E(\omega,0)+E(\omega,\pi)\right)}{4g^{4/3}P^{1/3}} \tag{34}$$

$$C_m = \frac{\omega^5 P^{2/3}\left(E(\omega,0)-E(\omega,\pi)\right)}{4g^{7/3}M}. \tag{35}$$

These estimates provide very close values of the Kolmogorov constants for all the series of Table 1 with the only exception of 'the almost isotropic' run `sw330` for the second Kolmogorov constant C_m. Fig. 9 gives the first Kolmogorov constant $C_p \approx 0.21 \pm 0.01$ (slightly lower values for initially narrow distributions) and $C_m \approx 0.08 \pm 0.02$ for all the runs except `sw330` (cf. figs.9*b,d* for 'narrow' `sw030` and 'wide' `sw230`).

The analytic estimate gives very close result $C_p = 0.219$ (Zakharov, 2010, eq.4.33). Numerical simulations by Lavrenov et al. (2002); Pushkarev et al. (2003); Badulin et al. (2005a) missed a factor of 2 in definitions of the Kolmogorov constants (cf. our definitions 4-6 and eqs. 4.29, 4.30 in Zakharov, 2010). Taking this into account, one has the reported values $0.151 < C_p < 0.162$; $0.105 < C_m < 0.121$ in Lavrenov et al. (2002, Table 1), $0.16 < C_p < 0.23$; $0.09 < C_m < 0.14$ in Pushkarev et al. (2003, eqs. 5.3, 5.6, 5.8) and $0.19 < C_p < 0.20$ in Badulin et al. (2005a). The first experimental attempt to evaluate the first Kolmogorov constant by Deike et al. (2014) presented value $C = 1.8 \pm 0.2 \approx 2\pi C_p$, i.e. 2π times bigger counterpart of C_p.

While the estimates of the Kolmogorov's constants for the swell look consistent the numerical solutions differ essentially from the approximate weakly anisotropic KZ solution (6). The directional spreading cannot be described by the only angular harmonics as in (6), higher-order corrections are clearly seen in figs.7 as side-lobes. Nevertheless, the robustness of the estimates of the second Kolmogorov constant C_m provides a good reference for estimates of the spectra anisotropy.

The estimates of C_m for `sw330` (fig. 9*f*) demonstrate a specific nonstationarity of the swell solution in terms of wave momentum flux while the first Kolmogorov constant C_p (fig.9*f*) show relevance of the stationary KZ solutions to the swell problem.

4 Discussion. Swell and ocean environment

Results of our simulations showed their fairly good correspondence to findings of the theory of wave (weak) turbulence. Relevance of these results to experimental facts seems to be a logical close of this work. The issue of relevance is two-fold. First, our results can help in explaining effects which interpretation in terms of alternative approaches (mostly, within linear theory) is questionable. Secondly, one can formulate, or, at least, sketch cases where our approach becomes invalid or requires an extension. Both aspects are considered in the final section.

Attenuation in course of long term swell evolution is an appealing problem of the swell monitoring. We show that contribution of wave-wave interactions to this process can be important mostly at initial stages of swell evolution. The observed rates of swell attenuation in an open ocean cannot be treated within our approach for a number of reasons. First of all, the duration-limited setup of our simulations do not account for important mechanisms of frequency dispersion and spatial divergence due to sphericity of the Earth. These mechanisms can both contribute into swell attenuation together with wave-wave interactions and essentially contaminate results of observations. The intrinsic swell attenuation is, generally, small as compared to the effect of reduction (or amplification at large fetches) (see fig.2b in Ardhuin et al., 2009) which is accounted for within the linear model of geometrical optics whose validity is generally assumed for ocean swell.

Ocean swell for long times (fetches), becomes likely an important constituent of the ocean environment which can be heavily affected by relatively short wind-driven waves. We discuss the effect of swell amplification at rather low wind speeds and give tentative estimates based on the approach of this paper.

4.1 Swell attenuation within the kinetic equation

Dependence of wave height on time is shown in upper panel of fig. 10 (see also fig.2) for the runs of Table1. All the runs show quantitatively close evolution. Strong drop of up to 30% of initial value occurs within a relatively short time of about one day. An essential part of the wave energy leakage corresponds to this transitional stage at the very beginning of swell evolution when swell is tending very rapidly to self-similar asymptotics. Afterwards, the decay becomes much slower at following the power-law dependence of the self-similar solutions (22).

For comparison with other models, and available observations, the duration-limited simulations have been recasted into dependencies of fetch through the simplest time-to-fetch transformation (e.g. Hwang and Wang, 2004; Hwang, 2006):

$$x(s) = \int_0^s C_g(\omega_p(t))dt. \tag{36}$$

The equivalent fetch is estimated as a distance covered by a wave guide travelling with the group velocity of the spectral peak component. The corresponding dependencies are shown in bottom panel in fig.10. Two quasi-linear models by Ardhuin et al. (2009) and Babanin (2006) predict relatively slow attenuation at fetches in a 'near zone' less than 1000 km (approximately 1 day) and then gradual decay up to very few of the percentage points initial value at final distances about 18000 km where our model shows qualitatively different weak attenuation.

It should be noted that our model describes attenuation of the ocean swell 'on its own' due to wave-wave interactions without any external effects. Thus, the effect of an abrupt drop of wave amplitude at short time (fetch) should be taken into consideration above all others when discussing possible application of our results to swell observations and physical interpretation of the experimental results.

4.2 Swell and wind sea coupling. Arrest of weakly turbulent cascading

Extremely weak attenuation of swell due to wave-wave interactions provokes a question on robustness of this effect. A variety of physical mechanisms in the ocean environment can change the swell evolution qualitatively. The above discussion of swell attenuation presents a remarkable example of such transformation when dissipation becomes dominant. Tracking of swell events from space gives an alternative scenario of transformation when swell appears to be growing. Satellite tracks can comprise up to 30% of cases of growing swell 'most of them are not statistically significant' (Jiang et al., 2016). Nevertheless, a possible effect of wind-sea background on long ocean swell opens an important discussion in view of theoretical (Badulin et al., 2008b) and experimental (Benilov et al., 1974; Badulin and Grigorieva, 2012) results that demonstrate swell amplification by wind wave background.

As noted and shown above, evolution of swell can occur at different time scales for different physical quantities. Integrals of motion (energy, action, momentum) evolve at relatively large scales: frequency downshift and energy follows power-law dependencies $1/11$ ($\omega_p \sim t^{-1/11}$ and $E \sim t^{-1/11}$). The slow evolution is supported by interactions within a wave spectra that is close to an 'inherent' quasi-stationary state.

Oppositely, spectral shaping is evolving due to excursions from an 'inherent state' at much shorter scales that can be estimated following Zakharov and Badulin (2011, see eqs.21,22 therein). The nonlinear relaxation rate as defined by eqs.14-16 of the cited paper can be written as

$$\Gamma(\omega) = B\omega \left(\frac{\omega}{\omega_p}\right)^3 \mu^4 H(\omega,\theta). \tag{37}$$

Here B is a big dimensionless coefficient (e.g. $B = 22.5\pi \approx 70.7$ for an isotropic spectrum, see Zakharov and Badulin, 2011) and $H(\omega,\theta)$ is directional distribution function (32). The big coefficient B in (37) provides relatively fast relaxation of local excursions (in wave scales) from the slowly evolving 'inherent' swell, especially, in high frequency domain (factor $(\omega/\omega_p)^3$ in eq.37). Evidences of this relaxation can be seen in evolution of angular distribution of the run `sw330` where visible transformation of angular distribution is observed for all the duration of more than three weeks (fig.6): the non-self-similar background of the swell spectra is feeding the core of the spectral distribution.

A similar effect can be realized in the mixed sea when background of relatively short wind-driven waves feeds the swell. Total energy flux of the swell is decaying as rapidly as $dE/dt \sim t^{-12/11}$ and at sufficiently large time the associated direct cascading can be arrested by inverse cascading of wind-driven waves which fast relaxation to an 'inherent' swell ensures the swell feeding. This mechanism has been analyzed numerically (Badulin et al., 2008b) and showed its remarkable efficiency.

Simple estimates of possibility of the effect can be made in terms of balancing of two fluxes: direct cascade of swell and inverse cascade of wind-driven fraction. The swell energy leakage can be estimated from the weakly turbulent law (Badulin et al., 2007, eq.1.9) as follows

$$\left(\frac{dE}{dt}\right)_{direct} = \frac{E^3\omega_p^9}{\alpha_{swell}^3 g^4} = \frac{{\mu_{swell}}^6 C_{swell}^3}{\alpha_{swell}^3 g} \tag{38}$$

Here swell parameters are marked by proper subscripts: $C_{swell} = g/\omega_p$ – phase velocity of the spectral peal component, μ_{swell} – swell steepness by definition (15), and α_{swell} – self-similarity parameter (α_{ss} in Badulin et al., 2007). Similar conversion of sea state parameters to spectral flux can be done for the wind sea fraction (see sect.5.1 in Badulin et al., 2007, or Table 1 in Gagnaire-Renou et al. (2011))

$$\left(\frac{dE}{dt}\right)_{inverse} \approx C_w \left(\frac{\rho_a}{\rho_w}\right)^3 \frac{U_{10}^3}{\alpha_{wind}^3 g} \tag{39}$$

where coefficient $C_w = O(1)$ is introduced as soon as the conversion is based on dimensonal analysis and generalization of experimental results (Toba, 1972). A counterpart of α_{swell}, the self-similarity parameter α_{wind} is approximately two times less in magnitude (Badulin et al., 2007). Thus, condition of balance of fluxes assotiated with different fractions of the mixed sea says

$$2C_w \frac{\rho_a}{\rho_w} \frac{U_{10}}{C_{swell}} \approx \mu_{swell}^2 \tag{40}$$

For relatively short swell with period $T_p = 10$s ($\lambda \approx 150$m) and wind speed $U_{10} = 7$m/s one gets a critical swell steepness $\mu_{swell} \approx 0.03$. In other words, the mean-over-ocean wind 7m/s can balance (arrest) direct cascading of rather steep swell and,

hence, provoke a growth of the swell due to absorbing short wind-driven waves. Evidently, this simple balance model gives very tentative estimate of the effect. Nevertheless, visual observations (Badulin and Grigorieva, 2012) and satellite data (Jiang et al., 2016), in our opinion, provide telling arguments for this phenomenon. Thus, 'negative dissipation' of swell (in the words of Jiang et al., 2016) could find its explanation within the simple model.

The simple estimate (40) shows a limited value of our 'pure swell' model for ocean environment. Potentially, the effect of even light wind on long-term propagation of swell can change the result qualitatively. Our pilot numerical studies (see also Badulin et al., 2008b) show importance of the swell and wind-sea coupling. This effect will be detailed in our further studies.

5 Conclusions

We presented results of sea swell simulations within the framework of the kinetic equation for water waves (the Hasselmann equation) and treated these properties within the paradigm of the theory of weak turbulence. A series of numerical experiments (duration-limited setup, WRT algorithm) has been carried out in order to outline features of wave spectra in a range of scales usually associated with ocean swell, i.e. wavelengths larger than 100 meters and duration of propagation up to $2 \cdot 10^6$ seconds (more than 23 days). It should be stressed that the exact collision integral S_{nl} (nonlinear transfer term) has been used in all the calculations. Alternatively, mostly operational approaches, like DIA (Discrete Approximation Approach) can corrupt the results quantitatively and even qualitatively.

Key results of the study:

1. A strong tendency for self-similar asymptotics is demonstrated. These asymptotics are shown to be insensitive to initial conditions in terms of evolution of integral quantities (wave energy, momentum). Moreover, universal angular distributions of wave spectra at large times have been obtained for both narrow (initial angular spreading 30°) and almost isotropic initial spectra. Bi-modality of the spectral distributions in our simulations is found to be in agreement with previous numerical and experimental results (Banner and Young, 1994a; Ewans, 2001; Ewans et al., 2004). The universality of the spectral shaping can be treated as an effect of mode selection when very few eigenmodes of the boundary problem determines the system evolution. The inherent features of wave-wave interactions are responsible for this universality making the effect of initial conditions insignificant. Generally, the self-similar swell is co-existing with a background which is far from self-similar state;

2. The classic Kolmogorov-Zakharov (KZ) isotropic and weakly anisotropic solutions for direct and inverse cascades are shown to be relevant to slowly evolving sea swell solutions. Estimates of the corresponding KZ constants are found to agree well with previous analytical, numerical and experimental results. Thus, features of KZ solutions can be used as a reference for advanced approaches in the swell studies;

3. We show that an inherent peculiarity of the Hasselmann equation, energy and momentum leakage, can also be considered as a mechanism of the sea swell attenuation. This mechanism is beyond the today models of sea swell. At the same time, the energy decay rates of sea swell in the numerical experiments, generally, do not contradict the results of recent swell

observations and modelling. These studies based on satellite data and wave model hindcasting are focused mostly on 'far field' behavior of swell, generally, 1000 or more kilometers away from a stormy area. Our simulations show that a dramatic transformation of the swell occurs at shorter distances, in 'near field'. The essential swell energy losses, mostly due to wave-wave interactions, in the near field is an intriguing challenge for sea wave forecasting. Thus, fig.10 outlines different domains of our model relevance rather than the model relevance to the general problem of ocean swell attenuation;

4. Long term evolution of swell is associated with rather slow frequency downshift ($\omega_p \sim t^{-1/11}$) and energy attenuation ($E \sim t^{-1/11}$). Meanwhile, the decay of other wave field quantities is essentially faster: wave steepness is decaying as $\mu \sim t^{-5/22}$ and total spectral flux even faster $dE/dt \sim t^{-12/11}$. This point is of key importance in our analysis as far as we consider nonlinear cascades of wave energy as governing physical mechanism of swell evolution. As we showed in discussion, the weak direct cascade of swell can be arrested by relatively light wind and then swell can start to grow. In our opinion, this conclusion correlates with manifestations of swell amplification in satellite data (Jiang et al., 2016) and in visual observations (Badulin and Grigorieva, 2012). Thus, 'negative dissipation' of swell (in the words of Jiang et al., 2016) could find its explanation within the simple estimate (40) of sect.4.2;

5. The last conclusion uncovers deficiency of the duration-limited setup for the phenomenon of swell. An alternative setup of fetch-limited evolution ($\partial/\partial t \equiv 0, \nabla_{\mathbf{r}} \neq 0$) introduces dispersion of wave harmonics as a competing mechanism that can change the swell evolution dramatically. Recent advances in wave modelling (Pushkarev and Zakharov, 2016) makes the problem of spatial-temporal swell evolution feasible and specify the perspectives of our first step study. The theoretical background for the classic fetch-limited setup when solutions depend on the only spatial coordinate (i.e. $\partial/\partial x \neq 0, \partial/\partial y \equiv 0$) is sketched in sect. 2 of this paper. The one-dimensional model add an essential physical effect of wave dispersion. A passage to cylindrical coordinates allows us to consider an effect of spatial divergence in formally one-dimensional problem where solutions depend on radial coordinate but are still anisotropic in wavevector space. Self-similar solutions for this problem in the spirit of sect. 2 can be easily found and related to numerical results. All the prospective simulations require developing effective numerical approaches. In particular, high angular resolution (not worse than 5°) could be recommended for these studies. V. Geogjaev & V. Zakharov has developed such code recently (a talk at the meeting Waves in Shallow Water Environment, 2016, Venice). We plan to use it in the swell studies.

Acknowledgements. Authors are thankful for the support of the Russian Science Foundation grant No. 14-22-00174. Authors are indebted to Prof. Victor Shrira and Vladimir Geogjaev for discussions and valuable comments. Authors are also grateful Dr. Andrei Pushkarev for his assistance in simulations. Authors appreciate critical consideration of the first version of the paper by anonymous reviewers. Their constructive feedback lead to substantial revision of sects.3 and 4.

References

Ardhuin, F., Chapron, B., and Collard, F.: Observation of swell dissipation across oceans, Geophys. Res. Lett., 36, L06607, doi:10.1029/2008GL037030, 2009.

Ardhuin, F., Rogers, E., Babanin, A. V., Filipot, J.-F., Magne, R., Roland, A., van der Westhuysen, A., Queffeulou, P., Aouf, J.-M. L. L., and Collard, F.: Semiempirical Dissipation Source Functions for Ocean Waves. Part I: Definition, Calibration, and Validation, J. Phys. Oceanogr., 40, 1917–1941, doi:10.1175/2010JPO4324.1, 2010.

Babanin, A. V.: On a wave-induced turbulence and a wave mixed upper ocean layer, Geophys. Res. Lett., 33, L20 605, doi:10.1029/2006GL027308, 2006.

Badulin, S. I. and A. N. Pushkarev, D. Resio, V. E. Z.: Self-similarity of wind-wave spectra. Numerical and theoretical studies, in: Rogue Waves 2004, edited by Olagnon, M. and Prevosto, M., vol. 39, pp. 205–214, Editions IFREMER, Brest, 2004.

Badulin, S. I. and Grigorieva, V. G.: On discriminating swell and wind-driven seas in Voluntary Observing Ship data, J. Geophys. Res., 117, doi:10.1029/2012JC007937, 2012.

Badulin, S. I., Pushkarev, A. N., Resio, D., and Zakharov, V. E.: Direct and inverse cascade of energy, momentum and wave action in wind-driven sea, in: 7th International workshop on wave hindcasting and forecasting, pp. 92–103, Banff, October 2002, available at https://www.researchgate.net/publication/253354120_Direct_and_inverse_cascades_of_energy_momentum_and_wave_action_in_spectra_of_wind-driven_waves, 2002.

Badulin, S. I., Pushkarev, A. N., Resio, D., and Zakharov, V. E.: Self-similarity of wind-driven seas, Nonl. Proc. Geophys., 12, 891–946, 2005a.

Badulin, S. I., Pushkarev, A. N., Resio, D., and Zakharov, V. E.: Universality of wind-wave spectra and exponents of wind-wave growth, in: Geophysical Research Abstracts, vol. 7, p. 01515, EGU, 2005b.

Badulin, S. I., Babanin, A. V., Resio, D., and Zakharov, V.: Weakly turbulent laws of wind-wave growth, J. Fluid Mech., 591, 339–378, 2007.

Badulin, S. I., Babanin, A. V., Resio, D., and Zakharov, V.: Numerical verification of weakly turbulent law of wind wave growth, in: IUTAM Symposium on Hamiltonian Dynamics, Vortex Structures, Turbulence. Proceedings of the IUTAM Symposium held in Moscow, 25-30 August, 2006, edited by Borisov, A. V., Kozlov, V. V., Mamaev, I. S., and Sokolovskiy, M. A., vol. 6 of *IUTAM Bookseries*, pp. 175–190, Springer, ISBN: 978-1-4020-6743-3, 2008a.

Badulin, S. I., Korotkevich, A. O., Resio, D., and Zakharov, V. E.: Wave-wave interactions in wind-driven mixed seas, in: Proceedings of the Rogue waves 2008 Workshop, pp. 77–85, IFREMER, Brest, France, 2008b.

Badulin, S. I., Zakharov, V. E., and Pushkarev, A. N.: Simulation of wind wave growth with reference source functions, Geophysical Research Abstracts, 15, EGU2013–5284–1, 2013.

Balk, A. M.: On the Kolmogorov-Zakharov spectra of weak turbulence, Phys. D: Nonlin. Phenom., 139, 137–157, 2000.

Banner, M. L. and Young, I. R.: Modeling spectral dissipation in the evolution of wind waves. Part I: assessment of existing model performance, J. Phys. Oceanogr., 24, 1550–1570, 1994a.

Banner, M. L. and Young, I. R.: Modeling Spectral Dissipation in the Evolution of Wind Waves. Part I: Assessment of Existing Model Performance, J. Phys. Oceanogr., 24, 1550–1571, doi:10.1175/1520-0485(1994)024<1550:MSDITE>2.0.CO;2, 1994b.

Barber, N. F. and Ursell, F.: The Generation and Propagation of Ocean Waves and Swell. I. Wave Periods and Velocities, Philosophical Transactions of the Royal Society of London. Series A, Mathematical and Physical Sciences, 240, 527–560, http://www.jstor.org/stable/91425, 1948.

Barrenblatt, G. I.: Scaling, self-similarity, and intermediate asymptotics : Dimensional analysis and intermediate asymptotics, Plenum Press, New York/London, 1979.

Beal, R. C., Kudryavtsev, V. N., Thompson, D. R., Grodsky, S. A., Tilley, D. G., Dulov, V. A., and Graber, V. A.: The influence of the marine atmospheric boundary layer on ERS-1 synthetic aperture radar imagery of the Gulf Stream, J. Geophys. Res., 102, 5799–5814, 1997.

Benilov, A. Y., Kouznetsov, O. A., and Panin, G. N.: On the analysis of wind wave-induced disturbances in the atmospheric turbulent surface layer, Boundary-Layer Meteorol., 6, 269–285, 1974.

Benoit, M. and Gagnaire-Renou, E.: Interactions vague-vague non-linéaires et spectre d'équilibre pour les vagues de gravité en grande profondeur d'eau, in: Proc. 18th Congrès Français de Mécanique, Grenoble (France), 2007.

Bottema, M. and van Vledder, G. P.: Effective fetch and non-linear four-wave interactions during wave growth in slanting fetch conditions, Coastal Eng., 55, 261–275, 2008.

Bottema, M. and van Vledder, G. P.: A ten-year data set for fetch- and depth-limited wave growth, Coastal Eng., 56, 703–725, 2009.

Chen, K. S., Chapron, B., and Ezraty, R.: A Global View of Swell and Wind Sea Climate in the Ocean by Satellite Altimeter and Scatterometer, J. Atmos. Ocean. Technol., 19, 1849–1859, 2002.

Deike, L., Miquel, B., Gutiérrez, P., Jamin, T., Semin, B., Berhanu1, M., Falcon, E., and Bonnefoy, F.: Role of the basin boundary conditions in gravity wave turbulence, J. Fluid Mech., 781, 196–225, doi:10.1017/jfm.2015.494, 2014.

Delpey, M. T., Ardhuin, F., Collard, F., and Chapron, B.: Space-time structure of long ocean swell fields, J. Geophys. Res., 115, doi:10.1029/2009JC005885, 2010.

Donelan, M. A., Hamilton, J., and Hui, W. H.: Directional spectra of wind-generated waves, Phil. Trans. Roy. Soc. Lond. A, 315, 509–562, 1985.

Ewans, K., Forristall, G. Z., Prevosto, M. O. M., and Iseghem, S. V.: WASP West Africa Swell Project, Final report, Ifremer - Centre de Brest, Shell International Exploration and Production, B.V., 2004.

Ewans, K. C.: Observations of the Directional Spectrum of Fetch-Limited Waves, J. Phys. Oceanogr., 28, 495–512, 1998.

Ewans, K. C.: Directional spreading in ocean swell, in: The Fourth International Symposium on Ocean Wave Measurement and Analysis, ASCE, San Francisco, 2001.

Gagnaire-Renou, E., Benoit, M., and Forget, P.: Ocean wave spectrum properties as derived from quasi-exact computations of nonlinear wave-wave interactions, J. Geophys. Res., 2010.

Gagnaire-Renou, E., Benoit, M., and Badulin, S. I.: On weakly turbulent scaling of wind sea in simulations of fetch-limited growth, J. Fluid Mech., 669, 178–213, 2011.

Hasselmann, K.: On the nonlinear energy transfer in a gravity wave spectrum. Part 1. General theory, J. Fluid Mech., 12, 481–500, 1962.

Hasselmann, K., Ross, D. B., Müller, P., and Sell, W.: A parametric wave prediction model, J. Phys. Oceanogr., 6, 200–228, 1976.

Henderson, D. M. and Segur, H.: The role of dissipation in the evolution of ocean swell, J. Geophys. Res. Oceans, 118, 5074–5091, doi:10.1002/jgrc.20324, 2013.

Hwang, P. A.: Duration and fetch-limited growth functions of wind-generated waves parameterized with three different scaling wind velocities, J. Geophys. Res., 111, doi:10.1029/2005JC003 180, 2006.

Hwang, P. A. and Wang, D. W.: Field measurements of duration-limited growth of wind-generated ocean surface waves at young stage of development, J. Phys. Oceanogr., 34, 2316–2326, 2004.

Jiang, H., Stopa, J. E., Wang, H., Husson, R., Mouche, A., Chapron, B., and Chen, G.: Tracking the attenuation and nonbreaking dissipation of swells using altimeters, J. Geophys. Res. Oceans, doi:10.1002/2015JC011536, 2016.

Kahma, K. K. and Pettersson, H.: Wave growth in a narrow fetch geometry, Global Atmos. Ocean Syst., 2, 253–263, 1994.

Kantha, L.: A note on the decay rate of swell, OM, 11, 167–173, doi:10.1016/j.ocemod.2004.12.003, 2006.

Katz, A. V. and Kontorovich, V. M.: Drift stationary solutions in the weak turbulence theory, JETP Letters, 14, 265–267, 1971.

Katz, A. V. and Kontorovich, V. M.: Anisotropic turbulent distributions for waves with a non-decay dispersion law, Soviet Physics JETP, 38, 102–107, 1974.

Lavrenov, I., Resio, D., and Zakharov, V.: Numerical simulation of weak turbulent Kolmogorov spectrum in water surface waves, in: 7th International workshop on wave hindcasting and forecasting, pp. 104–116, Banff, October 2002, available at https://www.researchgate.net/publication/312210314_Lavr_7th_Workshop, 2002.

Munk, W. H., Miller, G. R., Snodgrass, F. E., and Barber, N. F.: Directional Recording of Swell from Distant Storms, Phil. Trans. Roy. Soc. London, 255, 505–584, 1963.

Pettersson, H.: Wave growth in a narrow bay, Ph.D. thesis, University of Helsinki, http://ethesis.helsinki.fi/julkaisut/mat/fysik/vk/pettersson/, [ISBN 951-53-2589-7 (Paperback) ISBN 952-10-1767-8 (PDF)], 2004.

Phillips, O. M.: On the dynamics of unsteady gravity waves of finite amplitude, J. Fluid Mech., 9, 193–217, 1960.

Pushkarev, A. and Zakharov, V.: On nonlinearity implications and wind forcing in Hasselmann equation, ArXiv e-prints, 2015.

Pushkarev, A. and Zakharov, V.: Limited fetch revisited: Comparison of wind input terms, in surface wave modeling, Ocean Modelling, pp. –, doi:http://dx.doi.org/10.1016/j.ocemod.2016.03.005, http://www.sciencedirect.com/science/article/pii/S1463500316300026, 2016.

Pushkarev, A. N., Resio, D., and Zakharov, V. E.: Weak turbulent theory of the wind-generated gravity sea waves, Phys. D: Nonlin. Phenom., 184, 29–63, 2003.

Pushkarev, A. N., Resio, D., and Zakharov, V. E.: Second generation diffusion model of interacting gravity waves on the surface of deep water, Nonl. Proc. Geophys., 11, 329–342, sRef-ID: 1607-7946/npg/2004-11-329, 2004.

Snodgrass, F. E., Groves, G. W., Hasselmann, K. F., Miller, G. R., Munk, W. H., and Powers, W. H.: Propagation of Ocean Swell across the Pacific, Phil. Trans. Roy. Soc. London, 259, 431–497, 1966.

Toba, Y.: Local balance in the air-sea boundary processes. Part I. On the growth process of wind waves, J. Oceanogr. Soc. Japan, 28, 109–121, 1972.

Toffoli, A., Onorato, M., Bitner-Gregersen, E. M., and Monbaliu, J.: Development of a bimodal structure in ocean wave spectra, J. Geophys. Res., 115, doi:10.1029/2009JC005495, 2010.

Tracy, B. and Resio, D.: Theory and calculation of the nonlinear energy transfer between sea waves in deep water, WES Rep. 11, US Army, Engineer Waterways Experiment Station, Vicksburg, MS, 1982.

Webb, D. J.: Non-linear transfers between sea waves, Deep Sea Res., 25, 279–298, 1978.

Young, I. R.: Directional spectra of hurricane wind waves, J. Geophys. Res., 111, doi:10.1029/2006JC003 540, 2006.

Young, I. R., Hasselmann, S., and Hasselmann, K.: Computations of the response of a wave spectrum to a sudden change in wind direction, J. Phys. Oceanogr., 17, 1317–1338, 1987.

Young, I. R., Verhagen, L. A., and Banner, M. L.: A note on the bimodal directional spreading of fetch-limited wind waves, J. Geophys. Res., pp. 773–778, doi:10.1029/94JC02218, 1995.

Young, I. R., Babanin, A. V., and Zieger, S.: The Decay Rate of Ocean Swell Observed by Altimeter, J. Phys. Oceanogr., 43, 2322–2333, 2013.

Zakharov, V. E.: Statistical theory of gravity and capillary waves on the surface of a finite-depth fluid, Eur. J. Mech. B/Fluids, 18, 327–344, 1999.

Zakharov, V. E.: Theoretical interpretation of fetch limited wind-driven sea observations, Nonl. Proc. Geophys., 12, 1011–1020, 2005.

Zakharov, V. E.: Energy balance in a wind-driven sea, Phys. Scr., T142, 014 052, doi:10.1088/0031-8949/2010/T142/014052, 2010.

Zakharov, V. E. and Badulin, S. I.: On Energy Balance in Wind-Driven Seas, Doklady Earth Sciences, 440, 1440–1444, 2011.

Zakharov, V. E. and Filonenko, N. N.: Energy spectrum for stochastic oscillations of the surface of a fluid, Soviet Phys. Dokl., 160, 1292–1295, 1966.

Zakharov, V. E. and Pushkarev, A. N.: Diffusion model of interacting gravity waves on the surface of deep fluid, Nonl. Proc. Geophys., 6, 1–10, 1999.

Zakharov, V. E. and Zaslavsky, M. M.: Kinetic equation and Kolmogorov spectra in the weak-turbulence theory of wind waves, Izv. Atmos. Ocean. Phys., 18, 970–980, 1982.

Zakharov, V. E., Lvov, V. S., and Falkovich, G.: Kolmogorov spectra of turbulence. Part I, Springer, Berlin, 1992.

Zakharov, V. E., Korotkevich, A. O., Pushkarev, A. N., and Resio, D.: Coexistence of Weak and Strong Wave Turbulence in a Swell Propagation, Phys. Rev. Lett., 99, 2007.

Zakharov, V. E., Badulin, S. I., Hwang, P. A., and Caulliez, G.: Universality of Sea Wave Growth and Its Physical Roots, J. Fluid Mech., 708, 503–535, doi:10.1017/jfm.2015.468, 2015.

Zaslavskii, M. M.: Nonlinear evolution of the spectrum of swell, Izv. Atmos. Ocean. Phys., 36, 253–260, 2000.

Table 1. Initial parameters of simulation series

ID	Θ	N ($m^2 \cdot s$)	H_s (m)
`sw030`	30°	0.720	4.63
`sw050`	60°	0.719	4.6
`sw170`	180°	0.714	4.74
`sw230`	240°	0.721	4.67
`sw330`	330°	0.722	4.79

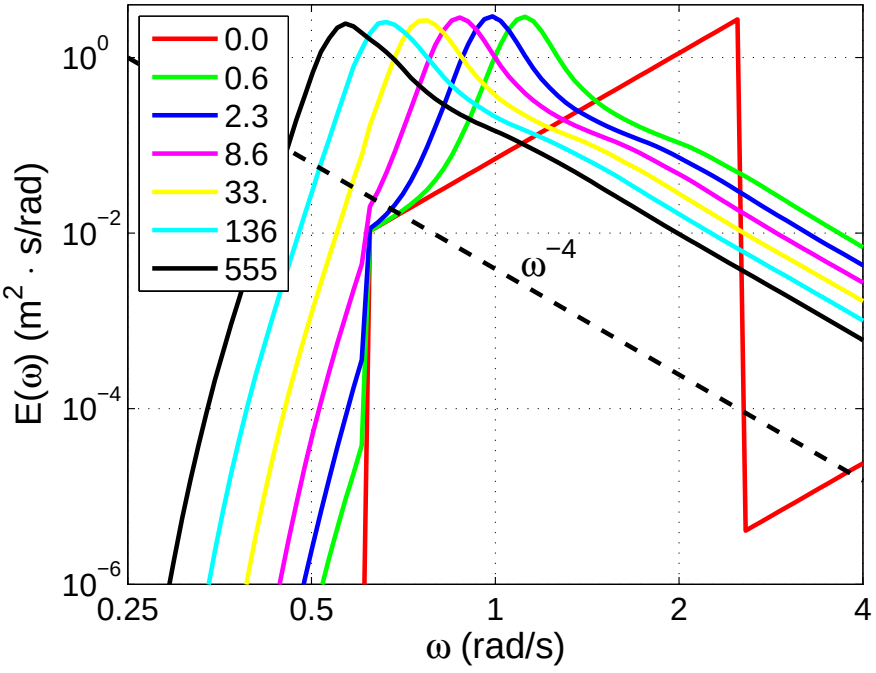

Figure 1. Frequency spectra of energy at different times (legend, in hours) for the case sw330 ($\Theta = 330°$).

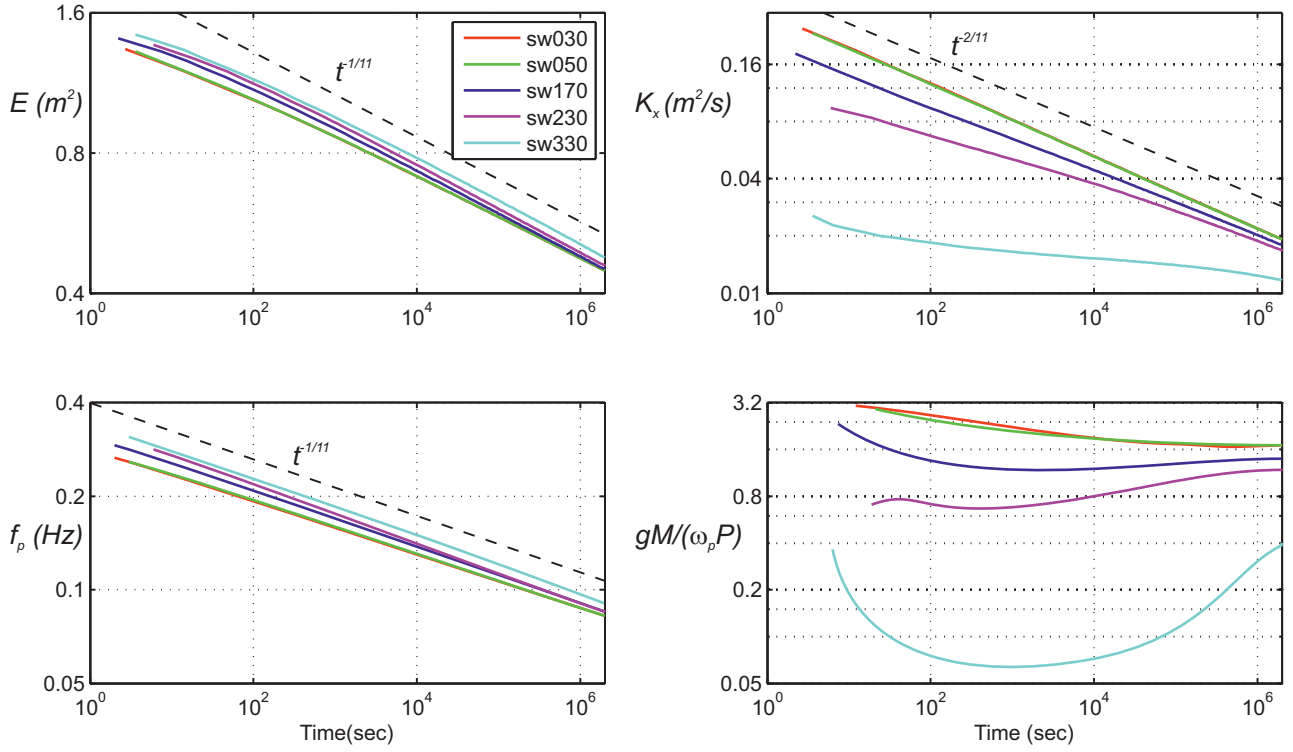

Figure 2. Evolution of wave parameters for runs of Table 1 (in legend): *a)* – total energy E; *b)* -total wave momentum M; *c)* – frequency $f_p = \omega_p/(2\pi)$ of the energy spectra peak; *d)* – estimate of parameter of anisotropy A (26). Dashed lines show asymptotic power laws (22,24)

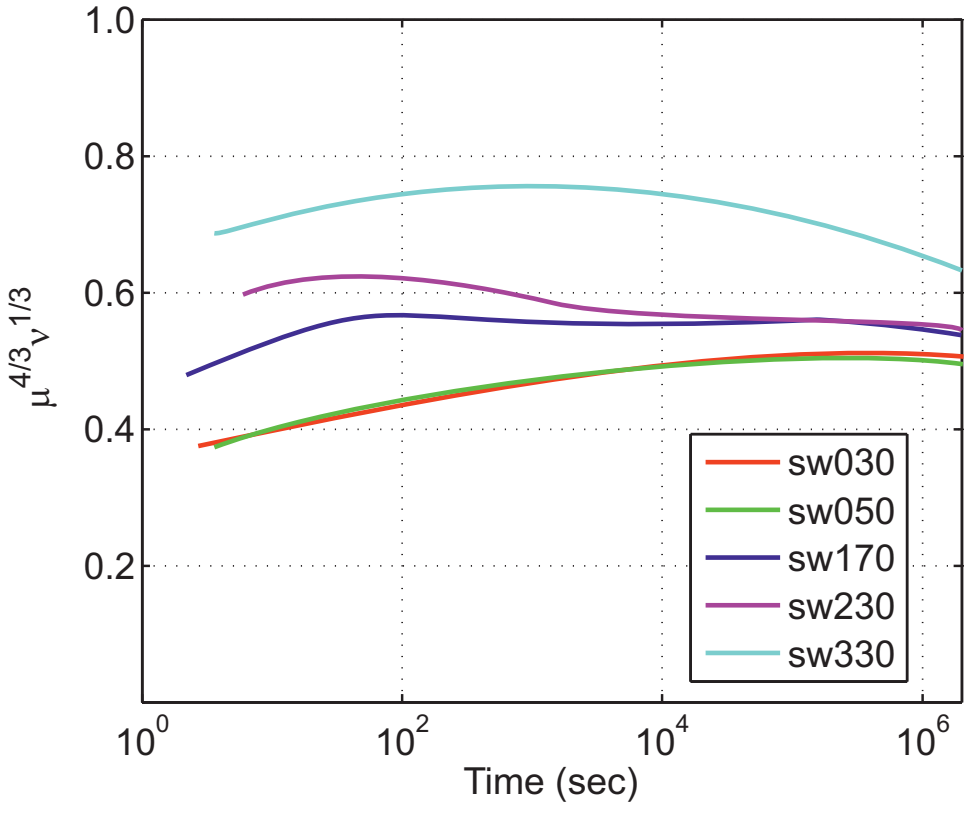

Figure 3. Evolution of the left-hand side of the invariant (14) $(\mu^4\nu)^{1/3}$ for runs of Table 1 (in legend).

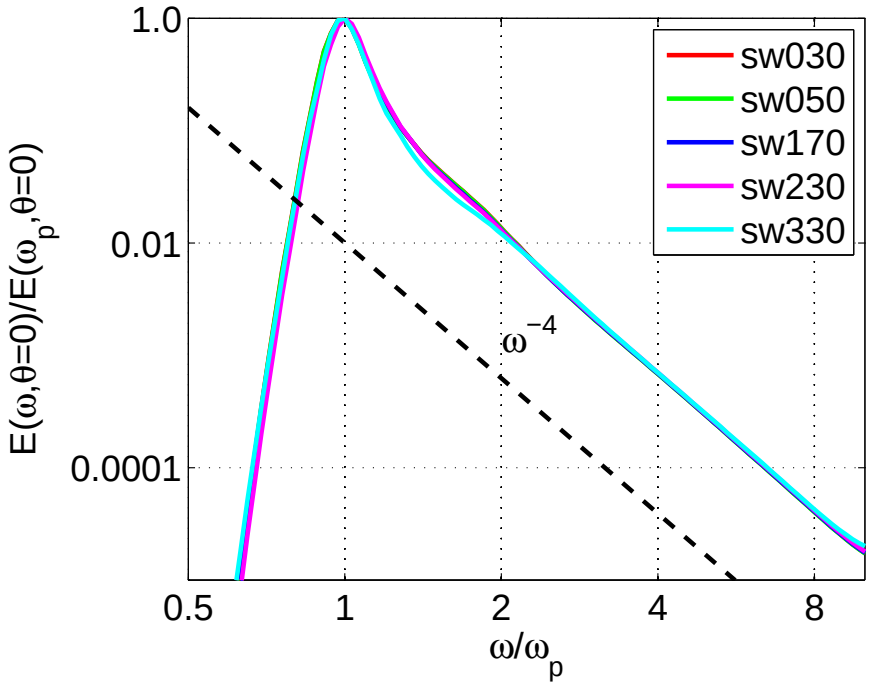

Figure 4. Normalized frequency spectra for direction $\theta = 0^\circ$ after 11.5 days (approximately 10^6 seconds) of swell evolution for runs of Table 1 (see legend).

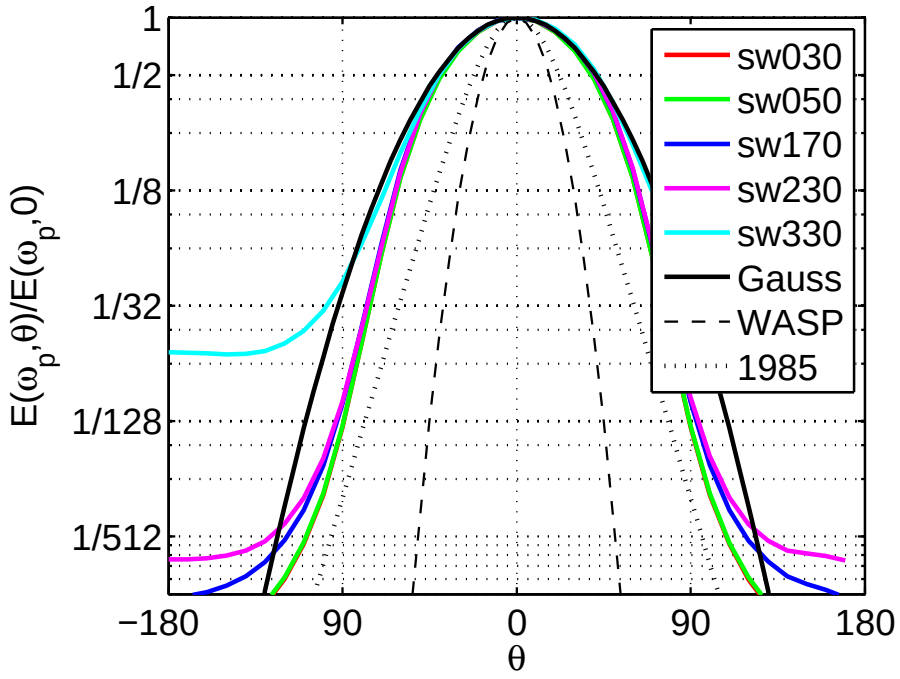

Figure 5. Normalized dependence of swell energy spectra on angle at peak frequency ω_p after 11.5 days (approximately 10^6 seconds) of swell evolution for runs of Table 1 (see legend). Dashed line – Gaussian distribution (29) with dispersion $\sigma_\Theta = 35^\circ$; dotted – growing sea (30) and eq.9.1-9.2 of Donelan et al. (1985); dashed – wrapped-normal fit of Ewans et al. (2004, Table 11.2, fig.11.8 in).

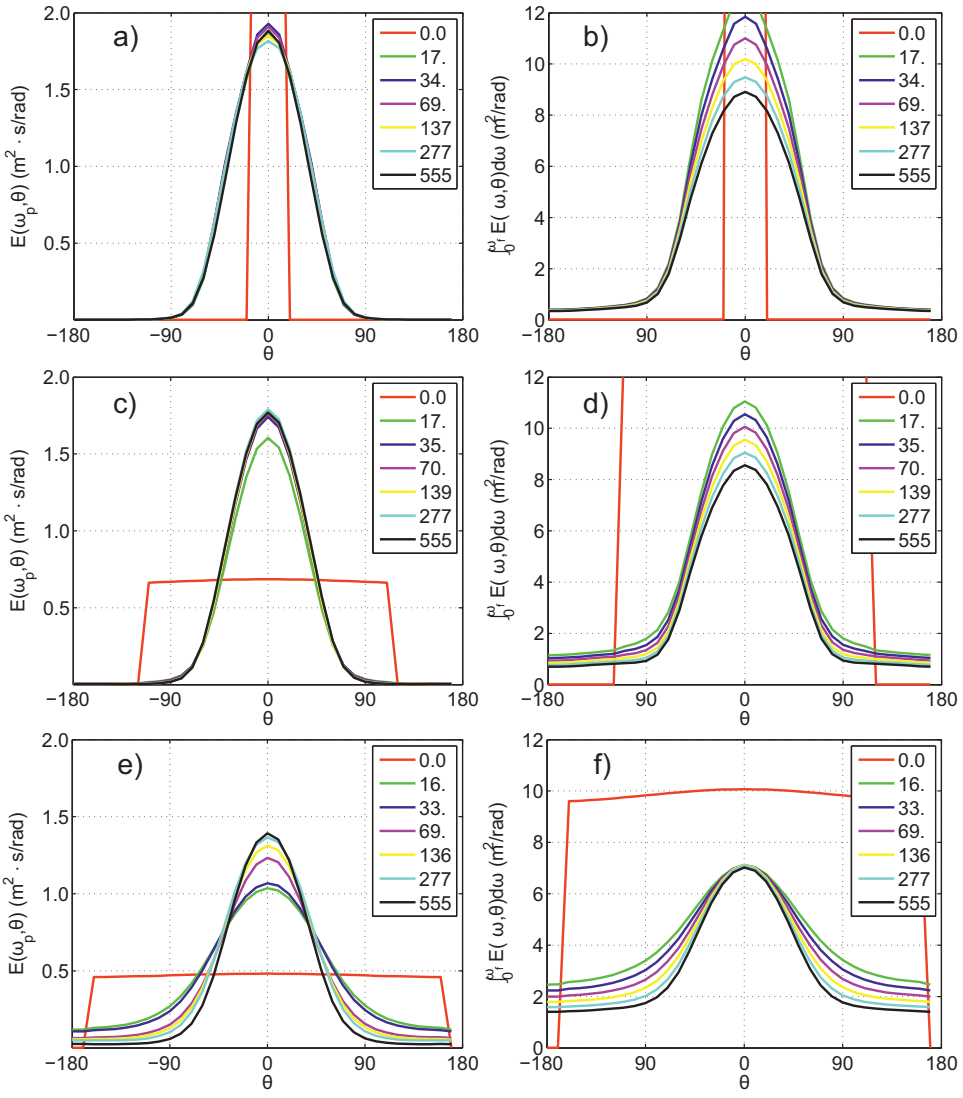

Figure 6. Angular spreading of the swell spectra at different times (in hours, see legend). Left column – wave spectra at peak frequency, right – integral of wave spectra in frequency as function of direction. *a,b)* – run sw030 of Table 1 – strong initial anisotropy; *c,d)* – run sw230 – weak anisotropy; *e,f)* – 'almost asitropic' run sw330.

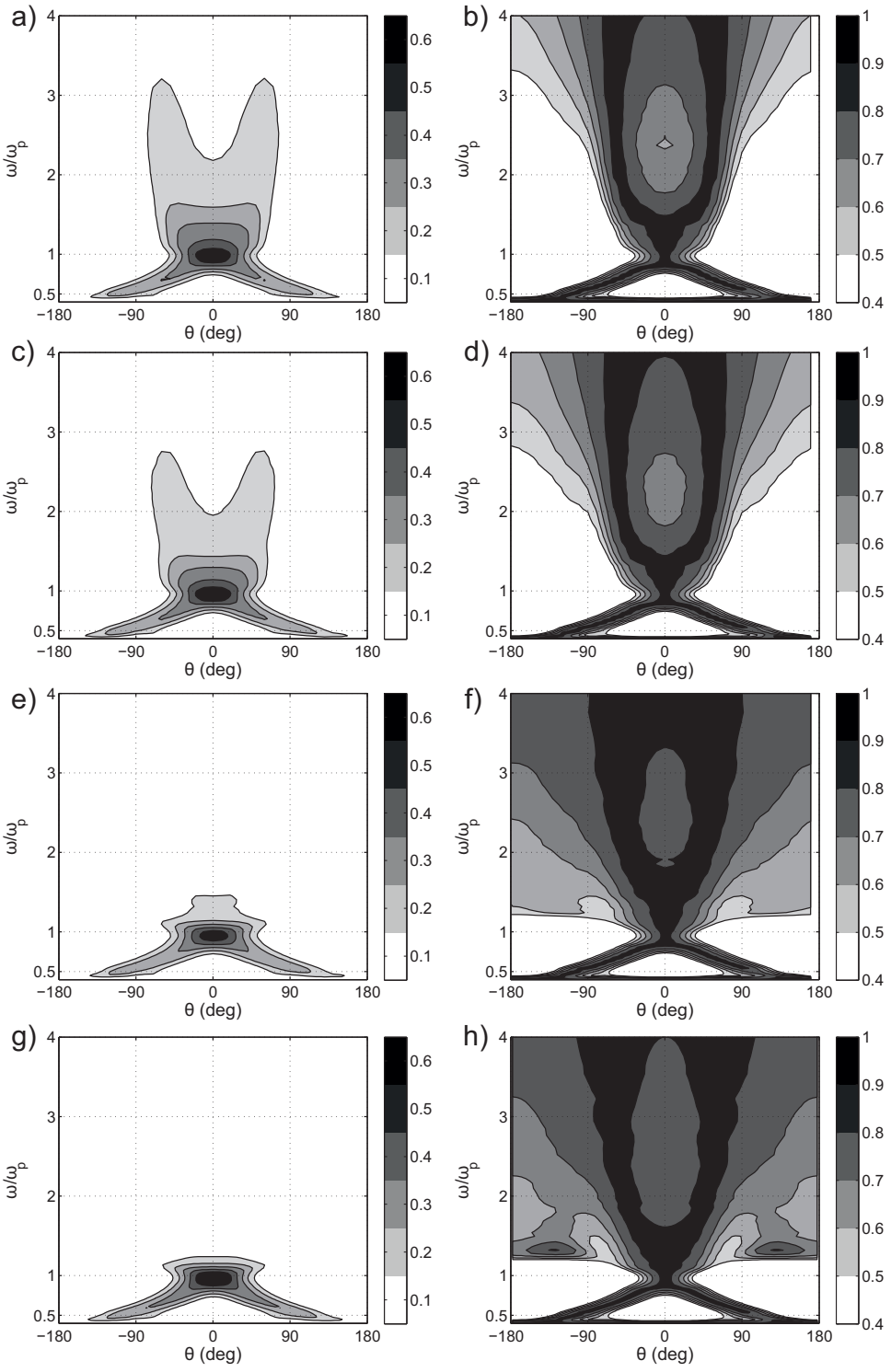

Figure 7. Isolines of spreading functions for different runs (see Table 1) *a,b)* – `sw030`; *c,d)* – `sw170`; *e,f)* – sw330; *g,h)* – run `sw330` with finer resolution in angle $\Delta\theta = 5^\circ$. Left column – definition (32), right – (33).

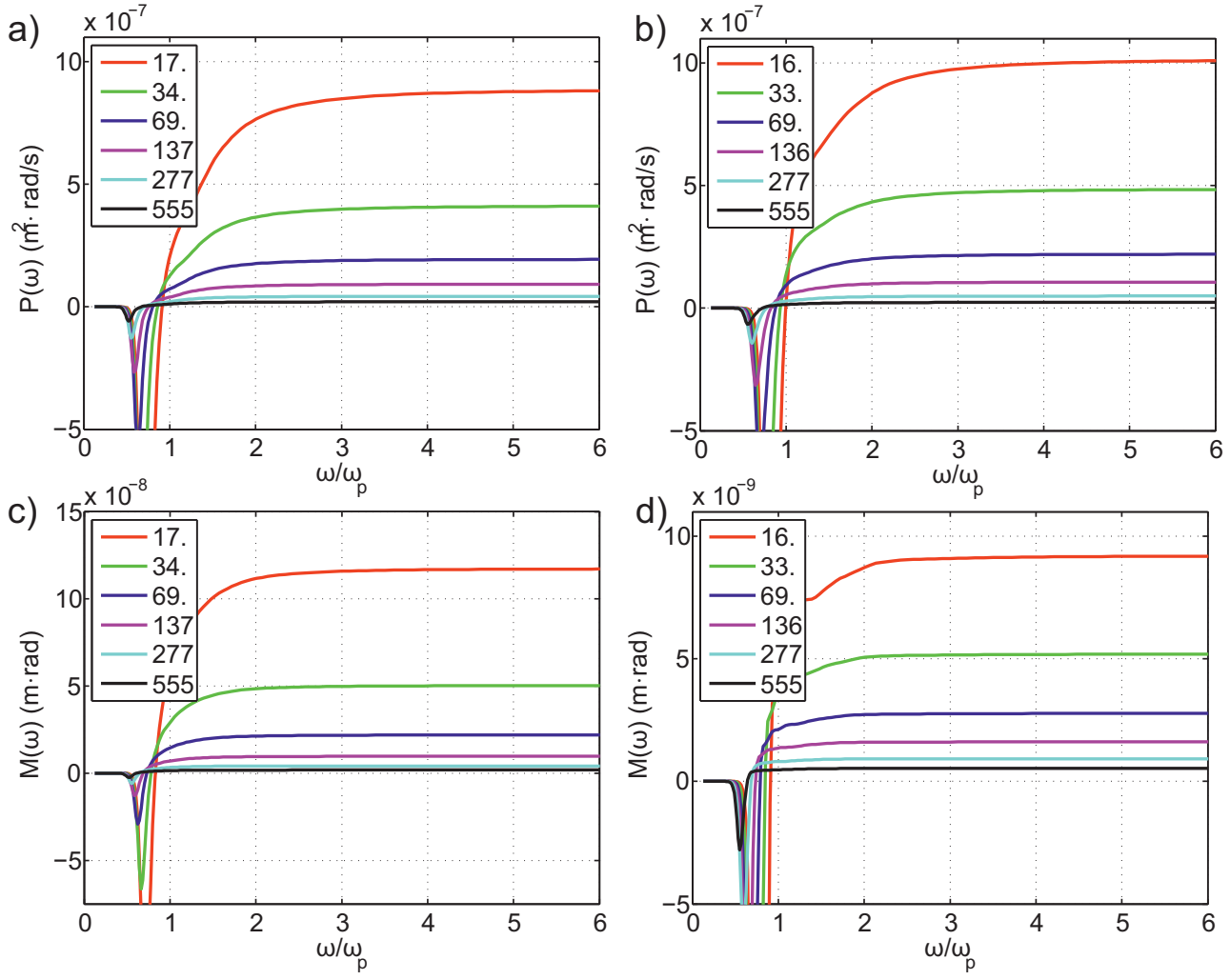

Figure 8. Top raw – spectral fluxes of energy for series `sw030` *(a)* and `sw330` *(b)*, bottom raw – spectral fluxes of momentum for series `sw030` *(c)* and `sw330` *(d)* at different times (legend, in hours).

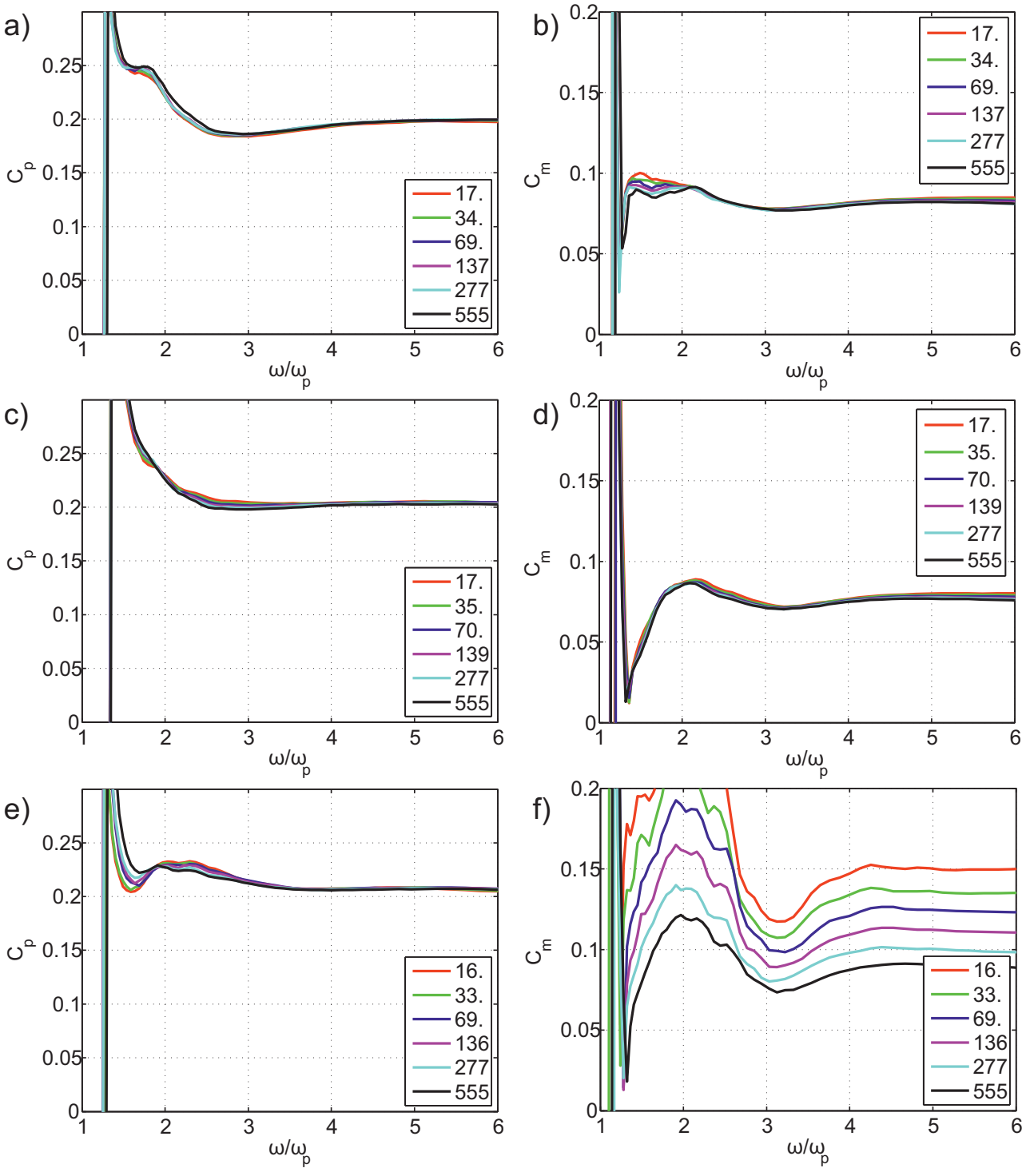

Figure 9. Left – estimates of the first Kolmogorov constant C_p, right – estimates of the second Kolmogorov constant C_m for the approximate anisotropic KZ solution (6). *a,b)* – run `sw030`; *c,d)* – `sw230`; *e,f)* – `sw330`. Time in hours is given in legend.

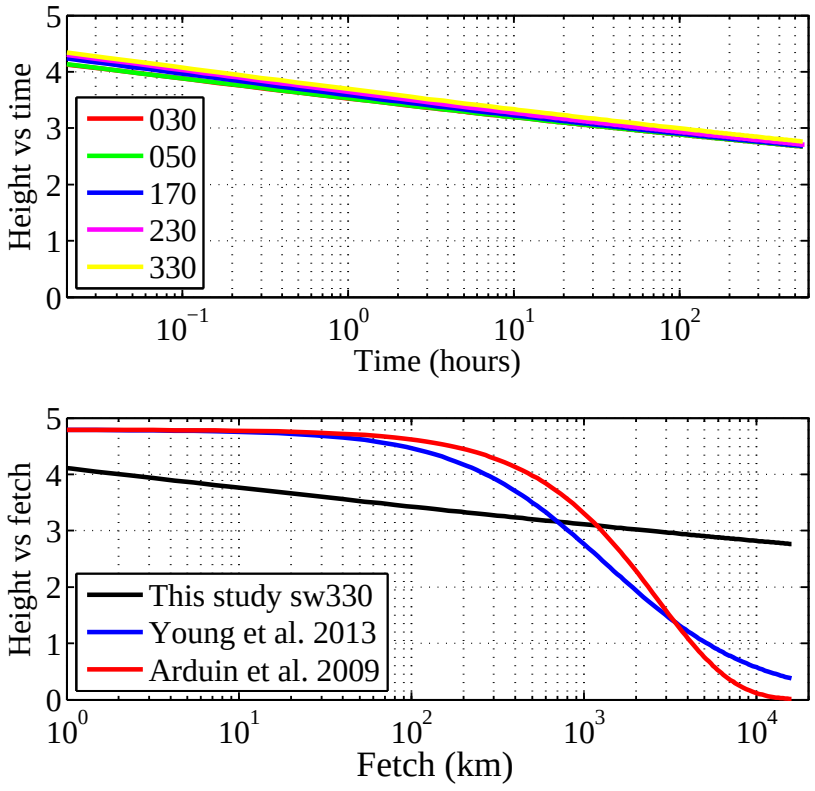

Figure 10. Top – dependence of significant wave height H_s on time for cases of Table 1. Bottom – attenuation of swell for models Ardhuin et al. (2009); Young et al. (2013) and one of this paper (see ledend). Results of duration-limited simulations are recasted into dependencies on fetch by simple transformation (36).

Answers to referee #1

Authors are grateful to the referee for attentive reading of the manuscript and valuable comments and suggestions. The authors took all these comments into account when preparing the revised version. Many changes are made in the text, almost all the figures have been re-drawn, additional numerical runs have been carried out as recommended by the referee for longer duration and with higher directional resolution. Ten new references appeared in the paper bibliography. Our answers follow the reviewer's report.

Major remarks:

1. The authors realizes severe limitations of the duration-limited setup in the problem of ocean swell. Nevertheless, even this extremely restrictive model show quite rich physics: self-similarity of swell evolution, universality of spectral shaping, bi-modality of directional spreading. Limitations of the duration-limited setup are now emphasized in many parts of the text (e.g. 3/17-25 Page/Line). Everywhere in the text we stress robustness of the effects of wave-wave interactions and present prospective plans for more realistic models of swell evolution in time and space where wave dispersion and spatial divergence play important roles. We also note resemblance of our results with previous numerical and experimental findings (e.g. Banner & Young, 1994; Ewans *et al.*, 2004);

2. The second point concerns the different phases of swell decay in the form of near- field and far-field. We agree that the near-field behavior of the ocean swell is extremely difficult to explore experimentally. This is why we consider our results on the role of wave-wave interactions in the near field as important. Discussion of directional spreading of swell is now extended. Illustrations are given both for narrow and wide directional distributions (figs.6,7). Swell attenuation in fig.10 is presented for all the runs of Table 1: angular spreading has no essential effect on rate of wave energy leakage. At the same time, initially wide spectra (e.g. run sw330) demonstrate quite strong transformation of angular spreading (fig.7) and essential deviations from the stationary KZ reference in terms of the second Kolmogorov constant C_m (fig.9f);

3. We do not consider the mechanism of wind wave absorption by swell as hypothetical. This effect has been discussed for experimental data

(e.g. Pettersson, 2004; Young, 2006) and in numerical simulations of the Hasselmann equation (Badulin *et al.*, 2008). In the updated paper we analyze this physical effect as a competition of two spectral fluxes: direct cascade produced by swell and inverse cascade of wind-driven waves. Wind waves in this scheme are attempting to grow but are just feeding the swell because of relatively fast relaxation to the inherent swell state (see eq.37 for the relaxation rate). The concise estimate (eq.40) looks quite suggestive for possible experimental verification. The authors are grateful to the reviewer for addressing to works on swell evolution (e.g. Ewans *et al.*, 2004) that gave important experimental illustrations of our results.

Minor remarks (Page number/Line number):

1. **2/2 briefly explain the concept of e-folding**
   Explained in lines 2/2: 'Their e-folding scale (distance in which an exponentially decaying wave height decreases by a factor of e) about 4000 km is consistent with some today results...';

2. **2/5 elaborate on the algebraic law, for which process is such a law made.**
   Now 2/6. We added comments on the model deficiency. The mentioned model relies upon a number of questionable hypothesis and empirical observations and cannot be incorporated straightforwardly into existent wave models in a mathematically consistent way;

3. **2/10 I disagree with the generality of the statement that swell is considered a superposition of sinusoidal components without interaction. Maybe in the time of Barber and Ursell (1948), and Snodgrass (1966) and before the time of 3G-wave models. Although I agree that the DIA in the WAM model is not a nice example due to its limitations.**

   We made the statement less radical (2/14): 'at most' instead of 'generally'. Unfortunately, the simplistic treatment of the swell is dominating today in time of 3G-wave models. We may refer to the feedback of the associate editor of Journal of Geophysical Research (the very first version of our paper has been rejected from JGR as it is mentioned in the submission form of NPG). Prof. Bruno Castelle wrote:

'Swell is rather unidirectional and monochromatic once it travels outside the storm area, the resonant interactions for such conditions should therefore be negligible, in contrast with your numerical experiments using a 'rectangular' spectral distribution'.

One of the referees of the JGR continues:

'As these waves propagate away from the storm generation site, frequency dispersion means that they separate out into almost monochromatic wave trains of the same frequency. These single frequency waves then propagate across oceanic basins and gradually decay.'

Thus, the hypotheses and the very first physical models of the ocean swell of brilliant papers by Barber and Ursell (1948), Snodgrass et al. (1966) are still alive without critical revision and without attentive reading of important parts of these works (e.g. sect.8 of Snodgrass et al., 1966);

4. **2/14 Briefly explain concept of e-folding**
   It is explained above (2/2 both in the paper and in the reviewer notes);

5. **2/15 You may reference to Kantha (2006) here concerning theories about swell decay.**
   Thank you, it is just to the point (2/5);

6. **2/21 Which other motions are meant here?**
   The issue is detailed, a reference is added (2/25);

7. **2/33 Add assumption of deep water and also note corresponding period range of 10 s–16 s**
   Thank you, done (3/2);

8. **3/9 A useful reference here is Delpey et al., 2009**
   Thank you for the useful link. It is cited now (3/16);

9. **3/10 Note that wave dispersion and spatial divergence are considered important in ocean scale swell propagation, although for distances over 10.000 km convergence kicks in.**
   The authors agree. It is noted in the revised text (e.g. Introduction and Discussion);

10. **3/13 The swell heightening by a weak background wind is rather speculative, see comments in appropriate section. I would not yet consider this a significant problem from a practical point of view. From a theoretical point of view it is interesting to figure out exactly what is happening.**
    Effects of the swell 'eating' wind-driven waves are described in Young (2006); Kahma & Pettersson (1994) and reproduced numerically in Badulin *et al.* (2008). In this paper we just propose a tentative estimate of conditions when this effect can play. The discussion of this effect is extended, see sect.4.2 ;

11. **4/3 The scaling law (2) only works when spectra are self-similar, which may not be the case in nature.**
    It is not correct. The homogeneity property (2) is valid for any function $N(\mathbf{k})$. It is purely mathematical fact that can be checked easily by simple change of variables in the collision integral S_{nl};

12. **5/7 I would rather drop the very before preliminary. Otherwise, this result is not worth publishing yet.**
    You are right, thank you. Fixed in 5/9-10;

13. **8/1 The model setup should be specified in more detail. Just referencing to Badulin et al. 200X is insufficient. After some checking it appear that a 1-point model is used to mimic duration limited wave growth, see e.g. Eq.6 in Badulin et al. (2005). This is an important detail, especially since it violates the statement on page/line 3/10.**
    Description of the model setup is extended (see sect.3.1). We see no contradiction with the statement of 3/10 if we treat 1-point (in the words of the reviewer) and duration-limited setups as synonyms;

14. **8/8** 10° **resolution may be adequate, although no reasoning is shown to back this claim, for the present application where** 30° **is the smallest directional spreading. In am not convinced whether this is sufficient for ocean swells in nature, where directional spreading in the range of** $10^\circ - 15^\circ$ **are common. For such situations a directional resolution of** 5° **is usually recommended.**

Calculations with 5° resolution have been carried out for 'the most inconvenient' runs sw030 and sw330 for the duration $2{\cdot}10^6$s. No difference in evolution of integral parameters (energy, momentum, spectral peak period) is found while quantitative difference in angular distributions is visible for frequencies higher than the peak one (fig.7e-h). Comments and new figures are given in the paper version. Robustness of the two-lobe angular distribution is stressed in sect.3.4. The necessity of higher directional resolution is stressed in final lines of the paper (18/25);

15. **8/10 The equation has some problems. The square 2 is at the wrong location. Further, the variables on each side of the equal sign are inconsistent. I suggest to use $N(\mathbf{k}, \theta)$ in the left-hand side. The frequencies ω_l, ω_h are not specified.**
Thank you. The typo is corrected. The expression in terms of θ and ω for the spatial spectrum looks more transparent (the issue of $N(\mathbf{k}) =$ const). Comments to the eclectic presentation are given to explain our preferences (8/19);

16. **8/17 Explain concept of hyper-dissipation, just the key notion is sufficient.**
We added the comment in sect.3.1 (8/26 and below). In earlier versions of the code (Pushkarev *et al.*, 2003) the hyper-viscosity option has been used to guarantee stability of calculations at high frequencies. Later on it has been realized that calculations can be stable in absence of dissipation (free boundary conditions). The sufficiently strong dissipation does not essentially affect numerical solutions: dissipation is stronger – spectral magnitudes are lower, and the overall effect of the dissipation reaches a sort of saturation. The dissipation effect just absorbs a spectral cascade directed to small (infinitely small) wave scales. Free boundary conditions work in a similar way;

17. **8/19 Why mention here the number of 30 runs, whereas the table 1 only contains 5 entries? What happened with the other 25 runs?**
Initial conditions are now described for all the series after 9/3. We focused on runs of Table 1 that cover the full set of angles (effect of anisotropy is our key priority) and have no troubles with possible instability or too slow evolution;

18. **9/7 If 11 days is too short, why not extend the simulation longer? On the other hand, the earths oceans may be too small to see this effect in nature. This poses a conflict, in the applicability of these results. There is only a tendency to approach self-similar solutions.**
Calculations for our main series (Table 1) are extended to $2 \cdot 10^6$ s to better specify tendency of wave parameters (height, period) and spectral shapes to a self-similar behavior and to specify 'pure effect' of nonlinear transfer due to four-wave interactions. It appears again 'too short'. Anyway, the tendency to self-similarity is better than tendency to nowhere. 'The effect in nature' requires an advanced setup with wave dispersion and spatial divergence/convergence taken into account as the reviewer himself stressed;

19. **10/10 Which definition of sigma is used: the linear or the circular definition. Note that the latter is commonly used in wave model to quantify the directional spreading**
Linear definition (in degrees) of σ and θ is used everywhere in the text and in figures. Hope, it makes no problem for the paper potential readers;

20. **10/13 Take a look at Ewans (1998) and Olagnon et al. (2013) for realistic estimates of swell widths, these are close to your definition of directional narrowness of $\Theta = 30°$.**
Thank you for this reminder. We had the authentic report of Ewans *et al.* (2004) and now use it in the updated text. This work give extremely wide range of estimates of directional spreading. We knew about this report when preparing the first version of the paper but it seemed too radical in following linear model of swell propagation. Now both papers are cited in the context of angular spreading of swell (sects.3.3,3.4);

21. **11/15 Equation number (31) is missing here. Renumber all follow-up equations**
There are no references to this equation in the text below. We leave the equation unnumbered;

22. **11/18 There are also negative fluxes!**
You are right. We added 'negative' and 'positive' in the previous

paragraph when discussing the hybrid nature of swell solutions (13/9, 13/10);

23. **11/26 Why not provide the other estimates for the reader to judge whether the results of this study are consistent?**
The values are provided (14/1-6), a reference (Deike *et al.*, 2014) to an experimental estimate of C_p is added;

24. **12/14 (Likely, 14/24) I am still surprised by this statement that such attenuation has never been seen in nature. Is it the result of your model setup of using only a 1-point model and only duration limited wave growth?**
The effect of attenuation of swell has never been discussed as one observed in nature. Other 'visible' mechanisms of swell decay like spatial dispersion or dissipation are in the focus of swell studies. Moreover, the fact itself of non-conservation of wave energy and momentum is not accepted by majority of researchers (Janssen, 2004, p.182, comments to eq.4.20 or p.137, sect. *Conservation laws* in Komen *et al.* (1995)),

25. **12/25 I wonder whether the case shown in Figure 10 is properly chosen. Sw330 can hardly be seen as representative for ocean swell in nature. Why not use the case sw030 here to illustrate the point. Now, I am afraid that completely different types of spectra are inter-compared, leading to false interpretation.**
Figure 10 is re-drawn. Upper panel shows all runs of the series with no essential quantitative difference. Thus, our choice representative. See also comments to page 29 below;

26. **13/20 Although the algebra may be trivial, mention the starting point of this exercise**
It is given in more details in sect.4.2 now;

27. **13/32 This may appear an interesting result, but it is only valid within certain assumptions of self-similar spectra. I doubt that this condition holds in case of some wind growth. I expect that some local enhancement of spectral density will appear, which will not cause any effect on the low-frequency part. Having said that, only detailed numerical experiments**

can shed light on this issue. So, I welcome this hypothesis, but for now it do not (yet) believe in this consequence.
The effect is seen fairly well in previous numerical experiments (Badulin *et al.*, 2008). We also have new results on this effect and hope to publish them soon;

28. **14/1 I disagree with the choice of the word clearly, see my previous comment. It is only an hypothesis within some assumptions.**
Thank you. We deleted it (17/5);

29. **14/11 Also quantitatively?**
Thank you. Now *'quantitatively and even qualitatively'* (17/15);

30. **14/15 I disagree that this can be used as a benchmark for real ocean swells in view of the limited size of earths oceans. See comment 9/7.**
Thank you. Now *'features KZ solutions can be used as a reference'*... (17/29);

31. **14/25 I disagree that todays models do not account for this effect. In case of the DIA, the most common method for S_{nl4}, this may be crude or wrong, but it does something.**
Thank you. Now we say: *'This mechanism is beyond the today models of sea swell...'* (17/31). The problem can be addressed to the DIA, first, to uncover whether the models are accounting for this effect;

32. **14/25 I am not convinced that this near field effect has never been observed or noted. It is now too easy stated that this is a problem. Still, it is an interesting notion for further investigations**
We did not say 'never been observed and noted'. The today studies of swell from space do avoid discussion the near field effects and, thus, skip an essential physics of sea wave dynamics. The text is modified (bottom of p.17, top p.18);

33. **15/8 This is an interesting statement, but in view of comment 8/1 both dispersion and spatial divergence are important. Only a true 2-d spherical model of swell propagation over the oceans can shed light on this issue. It is disappointing that this notion is not mentioned by the authors.**

Ok, we turn our cards over. Perspectives of the study are given in more details now (18/19 and below);

34. **15/12 No clear recommendations are given for further studies. See also previous point, which is probably one of the most important steps forward.**
Thank you. Corrected, see previous note;

35. **16/11 This reference cannot be found on the workshop website, only the abstract resides there.**
It is a pity. Reference to ResearchGate source of the paper is added. Similarly, the same conference paper of Lavrenov *et al.* (2002) is put into supplement of the ResearchGate web-page of Badulin *et al.* (2002) and the corresponding reference is given. Unfortunately, Prof. Igor Lavrenov deceased in 2009 and its paper resides now at this web-page;

36. **16/32 The journal of Chen et al., 2002 is wrong. Please correct. Journal of Atmospheric and Oceanic Technology**
Thank you. Fixed;

37. **19 Table 1 only list 5 of the 30 cases. What are the remaining 25 cases?**
Parameters of simulations are described in more details in sect.3.1;

38. **20 The initial shape at $t = 0$ does not match with Eq. 23.**
We see no problem. Eq.23 (eq.25 now) gives spectral density of wave action $N(\mathbf{k})$ while Fig.1 shows evolution of energy frequency spectrum

$$E(\omega) = \int_{-\pi}^{\pi} \frac{2\omega^4 N(\mathbf{k}(\omega,\theta))}{g^2} d\theta$$

(see for refs. Badulin *et al.*, 2005, unnumbered equations after eq.30);

39. **20 The unit along the vertical axis is incomplete $\mathbf{m^2/(rad/s)}$**
Thank you. Corrected for two times longer evolution;

40. **22 How do you explain the significant mismatch in behavior for case sw330?**
Calculations are continued up to $2 \cdot 10^6$s, Figs.2,3 are redrawn. The explanation can be found in sect.3.2-3.5. The case is 'too isotropic' and non-self-similar background corrupts a bit the simple asymptotics;

41. **24 It is known that S_{nl4} is weaker in directions than in frequencies to show self-similar behavior. This was for instance noted in the directional response behavior of the spectrum after a change in wind direction. I do not think the 1984 and 1985 are proper examples. See also remark 10/30.**
We leave 1985 and added WASP from Ewans *et al.* (2004). Weakness of S_{nl4} in direction is misleading. The relaxation rate depends on magnitude of excursion. This is what we see in fig.6 for sw330. See also 10/30 – speculations on different scales of evolution due to wave-wave interactions;

42. **25 The scale of the vertical axis is inconsistent with the one in Figure 5.**
You are right. In fig.5 normalized (by value at $\theta = 0$) values for different runs are shown while in fig.6 we give absolute values at different times for the same run in order to demonstrate the phenomenon of relaxation to a universal (our hypothesis) angular distribution;

43. **27 I am surprised that case sw170 is used is as an example. This deviates from other choices. Please comment on or argue this choice. Also, note the small instability for $t = 1$ hour. Also note that also the negative fluxes tend to diminish. Also, argue choice of sw170 for this example. What happens for other choices? In general, the behavior of sw030 or sw050 is much more interesting in relation to real ocean swells. Although, it is of interest that even for initial broad spectra, S_{nl4} tends to force a uniform shape.**
This figure is re-drawn. Results are shown for two extreme cases sw030 and sw330;

    Sorry, we do not see any instability for red curves $t = 1$hr.

    We answered the question on negative fluxes (hybrid nature of swell evolution) in the note 11/18. Negative fluxes follow the same tendency as positive fluxes when solutions are tending to self-similar behavior. We see no reason to emphasize this point here.

    Thanks for your last phrase of this note. You stressed the very important finding of our work: S_{nl4} provides a uniform (we say universal) shapes of swell irrespectively to initial spectral distribution;

44. **28 Same comment in relation to choice of SW170**
Three cases are shown. The only outlier is sw330 for the second Kolmogorov constant C_m;

45. **29 I am surprised that for this figure sw330 is taken to compare with observations. Why not sw030 or sw050 as that is much closer to field data**
Re-drawn. All cases are shown. Time and coordinate axes are logarithmic now to see the 'near-field' better;

46. **29 There is an inconsistency between figure legend and body text concerning reference to Badulin.**
Thank you. The figure is re-drawn. Time and fetch axes are log-spaced now in order to demonstrate strong drop of wave heights in near zone (less than 1000 km). Curves are given for all runs of the series and show quite close behavior for different initial distributions.

References

Badulin, S. I., Korotkevich, A. O., Resio, D. & Zakharov, V. E. 2008 Wave-wave interactions in wind-driven mixed seas. In *Proceedings of the Rogue waves 2008 Workshop*, pp. 77–85. IFREMER, Brest, France.

Badulin, S. I., Pushkarev, A. N., Resio, D. & Zakharov, V. E. 2002 Direct and inverse cascade of energy, momentum and wave action in wind-driven sea. In *7th International workshop on wave hindcasting and forecasting*, pp. 92–103. Banff, October 2002, available at `https://www.researchgate.net/publication/253354120_Direct_and_inverse_cascades_of_energy_momentum_and_wave_action_in_spectra_of_wind-driven_waves`.

Badulin, S. I., Pushkarev, A. N., Resio, D. & Zakharov, V. E. 2005 Self-similarity of wind-driven seas. *Nonl. Proc. Geophys.* **12**, 891–946.

Banner, M. L. & Young, I. R. 1994 Modeling spectral dissipation in the evolution of wind waves. part i: Assessment of existing model performance. *J. Phys. Oceanogr.* **24** (7), 1550–1571.

Deike, L., Miquel, B., Gutiérrez, P., Jamin, T., Semin, B., Berhanu1, M., Falcon, E. & Bonnefoy, F. 2014 Role of the basin

boundary conditions in gravity wave turbulence. *J. Fluid Mech.* **781**, 196–225.

Ewans, Kevin, Forristall, George Z., Prevosto, Michel Olagnon Marc & Iseghem, Sylvie Van 2004 WASP West Africa Swell Project. Final report. Ifremer - Centre de Brest, Shell International Exploration and Production, B.V.

Janssen, P. A. E. M. 2004 *The Interaction of Ocean Waves and Wind*. Cambridge Univ. Press, New York, 300 pp.

Kahma, K. K. & Pettersson, H. 1994 Wave growth in a narrow fetch geometry. *Global Atmos. Ocean Syst.* **2**, 253–263.

Komen, G. J., Cavaleri, L., Donelan, M., Hasselmann, K., Hasselmann, S. & Janssen, P. A. E. M. 1995 *Dynamics and Modelling of Ocean Waves*. Cambridge University Press.

Lavrenov, I., Resio, D. & Zakharov, V. 2002 Numerical simulation of weak turbulent Kolmogorov spectrum in water surface waves. In *7th International workshop on wave hindcasting and forecasting*, pp. 104–116. Banff, October 2002, available at `https://www.researchgate.net/publication/312210314_Lavr_7th_Workshop`.

Pettersson, Heidi 2004 Wave growth in a narrow bay. PhD thesis, University of Helsinki, [ISBN 951-53-2589-7 (Paperback) ISBN 952-10-1767-8 (PDF)].

Pushkarev, A. N., Resio, D. & Zakharov, V. E. 2003 Weak turbulent theory of the wind-generated gravity sea waves. *Phys. D: Nonlin. Phenom.* **184**, 29–63.

Young, I. R. 2006 Directional spectra of hurricane wind waves. *J. Geophys. Res.* **111**, doi:10.1029/2006JC003540.

Answers to referee #2

The authors appreciate efforts of the reviewer and his/her valuable comments. The paper is significantly updated: almost all the figures have been re-drawn, additional numerical runs have been carried out as recommended by one of referee for longer duration and with higher directional resolution. Ten new references appeared in the paper bibliography. Our answers follow the reviewer's report.

1. **The simulations are made for a very long time scale; could higher order effect in the kinetic equation take place (e.g. five wave interactions?)**
   We do not discuss the effect of five-wave (and higher-order) interactions intentionally by a number of reasons.

   First, the solution itself of the four-wave (Hasselmann) kinetic equation for long time is a real computational problem. The five-wave extension of the equation is well-known (see sect.5 and eqs. 5.1, 5.2 Krasitskii, 1994) but the authors are not aware of attempts to solve it numerically.

   Secondly, the passage to the five-wave kinetic equation is 'of principal significance' in words of Krasitskii (1994). The account for five-wave interactions is violating the wave action conservation law (wave energy and momentum remain to be formal integrals of the extension) and, thus, makes the theoretical concept of the Kolmogorov-Zakharov cascading and power-law Kolmogorov's spectra inapplicable. The authors set a high value on the theoretical background in this paper;

   Finally, our principal goal was to stay within the today concept of wind wave and swell prediction where the four-wave Hasselmann equation plays a key role. Tentative estimates of the effect of five-wave interactions for low steepness swell ($\mu \simeq 0.01$) offer prospects of their rather small effect. Quite interesting issue of wave field short-crestedness at long times (e.g. Badulin *et al.*, 1996) is, evidently, beyond of the paper goals and the statistical theory of sea waves;

2. **Line 9, page 6: while discussing the two-lobe structure of the higher frequency part of the spectrum, the authors state that the appearance of such structure is generally discussed as an effect of wind. This is only partially true, indeed, the role of**

nonlinearity in the formation of the lobes has been already discussed in Toffoli, Alessandro, et al. "Development of a bimodal structure in ocean wave spectra." Journal of Geophysical Research: Oceans 115.C3 (2010).
Thank you. This note is extended by references to Pushkarev *et al.* (2003) and Toffoli *et al.* (2010). Note, that the latter paper presents results of simulations for rather short durations of very few hundreds peak periods, i.e. about one hour only for our swell parameters. An extensive discussion of the spectra bi-modality is given in sect.3.4 with references to experimental (Ewans, 2001; Ewans *et al.*, 2004) and numerical works (Banner & Young, 1994; Young *et al.*, 1995);

3. **in eq. (16) the letter ν has already been used for the degree of homogeneity of the wave action.**
Thank you. Symbol ν in (2) is changed to υ now;

4. **Please, comment more on the fact that the 'wave action is the only true integral of the kinetic equation'.**
Comments are given in the cited papers (Zakharov *et al.*, 1992; Pushkarev *et al.*, 2003);

5. **Please, explain what do the authors mean by 'free boundary condition' (line 15 page 8)**
A short comment is added (now line 25, p.8): 'Free boundary conditions were applied at the high-frequency end of the domain of calculations: generally, short-term oscillations of the spectrum tail do not lead to instability, i.e. the resulting solutions can be regarded as ones corresponding to condition of decay at infinitely small scales ($N(\mathbf{k}) \to 0$ when $|\mathbf{k}| \to \infty$).'

6. **How much the reduction of the wave energy (H_s) depend on the high frequency cut off in the simulations?**
We did not find difference when reduced number of frequency grid points from 128 to 112. This is mentioned in the updated text (line 1, p.9)

7. **English should be improved.**
Thank you. We did our best to make the paper readable

References

Badulin, S. I., Shrira, V. I. & Kharif, C. 1996 A model of water wave 'horse-shoe' patterns. *J. Fluid Mech.* **318**, 375–405.

Banner, M. L. & Young, I. R. 1994 Modeling spectral dissipation in the evolution of wind waves. part i: Assessment of existing model performance. *J. Phys. Oceanogr.* **24** (7), 1550–1571.

Ewans, Kevin, Forristall, George Z., Prevosto, Michel Olagnon Marc & Iseghem, Sylvie Van 2004 WASP West Africa Swell Project. Final report. Ifremer - Centre de Brest, Shell International Exploration and Production, B.V.

Ewans, K. C. 2001 Directional spreading in ocean swell. In *The Fourth International Symposium on Ocean Wave Measurement and Analysis, ASCE, San Francisco*.

Krasitskii, V. P. 1994 On reduced Hamiltonian equations in the nonlinear theory of water surface waves. *J. Fluid Mech.* **272**, 1–20.

Pushkarev, A. N., Resio, D. & Zakharov, V. E. 2003 Weak turbulent theory of the wind-generated gravity sea waves. *Phys. D: Nonlin. Phenom.* **184**, 29–63.

Toffoli, A., Onorato, M., Bitner-Gregersen, E. M. & Monbaliu, J. 2010 Development of a bimodal structure in ocean wave spectra. *J. Geophys. Res.* **115** (C03006).

Young, I. R., Verhagen, L. A. & Banner, M. L. 1995 A note on the bimodal directional spreading of fetch-limited wind waves. *J. Geophys. Res.* pp. 773–778.

Zakharov, V. E., Lvov, V. S. & Falkovich, G. 1992 *Kolmogorov spectra of turbulence. Part I*. Springer, Berlin.